

Model subgrid microscale interactions to holistically discretise stochastic partial differential equations

A. J. Roberts*

December 13, 2018

Abstract

Constructing discrete models of stochastic partial differential equations is very delicate. Here we use stochastic centre manifold theory to derive and support spatial discretisations of the nonlinear advection-diffusion dynamics of the stochastically forced Burgers' equation. The trick to the application of the theory is to divide the physical domain into finite sized elements by introducing insulating internal boundaries which are subsequently removed to fully couple the dynamical interactions between neighbouring elements. The crucial aspect of this work is that we explore how a multitude of subgrid microscale noise processes interact via the nonlinear dynamics within and between neighbouring elements to affect the macroscale dynamics. Noise processes with coarse structure across a finite element are the most significant noises for the discrete model. Their influence also diffuses away to weakly correlate the noise in the spatial discretisation. The nonlinear dynamics has two further consequences: the example additive forcing generates multiplicative noise effects in the discretisation; and effectively new noise sources are abstracted into the macroscale discretisation. The techniques and theory developed here may be applied to discretise many dissipative stochastic partial differential equations.

*Computational Engineering and Science Research Centre, Department of Mathematics & Computing, University of Southern Queensland, Toowoomba, Queensland 4352, Australia. <mailto:aroberts@usq.edu.au>

Contents

1	Introduction	2
1.1	Divide space into discrete finite elements	6
1.2	Model nonlinear stochastic dynamics	6
2	Stochastic centre manifold theory underpins modelling	9
3	Construct a memoryless normal form of diffusion	14
3.1	Iteration converges to the asymptotic series	15
3.2	Corrections from a simple residual	16
3.3	Some convolutions need to be separated	17
3.4	Diffusion correlates noise across space	20
3.5	Next nearest neighbour elements affect noise	23
4	Nonlinear dynamics have irreducible noise interactions	25
4.1	Separate products of convolutions	25
4.2	Odd noise highlights nonlinear noise interactions	27
4.3	Strong models of stochastic dynamics are complex	31
5	Stochastic resonance influences deterministic dynamics	34
5.1	Canonical quadratic noise interactions	34
5.2	Translate to a corresponding SDE	36
5.3	Transform the detailed strong model to be usefully weak. . . .	37
5.4	Consolidate the new noise	39
6	Conclusion	41
A	Local simple noise is impossible	42
	References	43

1 Introduction

I introduce a dynamical systems approach to constructing discrete models of stochastic partial differential equations (SPDEs) by illustrating the concepts, analysis and results for the definite example of the stochastically forced Burgers' equation. The aim is to use stochastic centre manifold (SCM) theory and techniques to ensure the accuracy, stability and efficiency of numerical discretisations of SPDEs. Due to the forcing over many length and time scales,

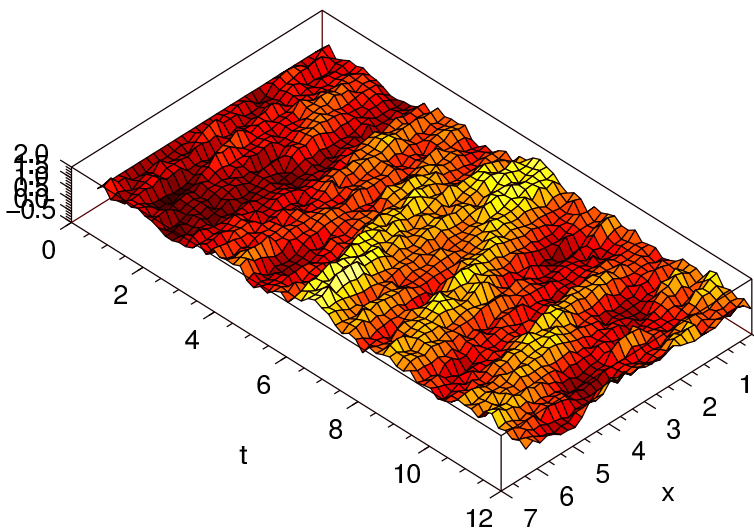


Figure 1: an example microscale simulation of one realisation of the stochastically forced Burgers' SPDE (1), with nonlinearity $\alpha = 3$ and noise intensity $\sigma = 1$. This simulation uses a fine space-time mesh with $\Delta x = \pi/16$ and $\Delta t = 0.01$ but plotted every 19th time step.

a SPDE typically has intricate spatio-temporal dynamics. Numerical methods to integrate stochastic *ordinary* differential equations are known to be delicate and subtle [29, e.g.]. We surely need to take considerable care for SPDEs as well [26, 59, e.g.] in order to model the subgrid microscale nonlinear interactions.

Furthermore, the sound methodology for modelling SPDEs presented here is likely to be needed to underpin multiscale modelling of physical systems in future applications [16, e.g.]. For example, the gap-tooth scheme of Kevrekidis et al. [23, 53, 54] is often implemented with particle simulators which are inherently stochastic within each simulation element. Hence connecting elements with stochastic microscale dynamics is as important as connecting elements with deterministic dynamics [52].

This article aims to build a bridge between physicists and engineers who need to solve problems in noisy systems and some tremendously useful stochastic theory. I seek the indulgence of probabilists for the necessarily somewhat simplistic treatment of their sophisticated theory.

The core theme of this article is the spatial discretisation of the non-dimensional stochastically forced Burgers' equation

$$\frac{\partial u}{\partial t} + \alpha u \frac{\partial u}{\partial x} = \frac{\partial^2 u}{\partial x^2} + \sigma \phi(x, t), \quad (1)$$

for a field $u(x, t)$ evolving in time t in one spatial dimension. This particular SPDE serves to introduce techniques required for many dissipative SPDEs. Givon et al. [24, p.R58] use a similar approach justified by the following:

Thus, much of the paper will be devoted to the development of model problems, and the underlying theoretical context in which they lie. Model problems are of central importance in order to make clear statements about the situations in which we expect the given algorithms to be of use, and in order to develop examples which can be used to test these algorithms. We do not state theorems nor give proofs—we present the essential ideas and refer to the literature for precise statement and rigorous analysis.

The Burgers' SPDE (1) explored in this article is a prototype example for many physically important SPDEs. Burgers' SPDE (1) incorporates the mechanisms of dissipation, u_{xx} , nonlinear advection/steepening, uu_x , controlled by the nonlinearity parameter α , and the stochastic forcing $\phi(x, t)$ controlled by the strength parameter σ . Da Prato et al. [15, 14] proved the existence and uniqueness of global solutions to Burgers' SPDE (1). Figure 1 shows one simulation of the stochastically forced Burgers' SPDE (1): observe the nonlinear advection of the noise peaks. In contrast the linear diffusion dynamics simulated in Figure 2 lacks the nonlinearity induced microscale interactions. One challenge resolved in Section 5 is to model any growth on the macroscale by accounting for the microscale interactions in the closure of the discretisation rather than in the simulation. That is, we aim to use macroscale space-time grids in the simulation, while accounting for the subgrid microscale interactions in the derivation of the discretisation. In essence we test a methodology for closure of macroscale discretisations through analysing subgrid microscale stochastic dynamics.

But even discretising linear SPDEs is subtle. For example, consider the forced diffusion equation obtained from Burgers' SPDE (1) with nonlinearity parameter $\alpha = 0$; see a simulation in Figure 2. The simplest finite difference approximation in space on a regular grid in x , say $X_j = jh$ for some constant grid spacing h , is

$$\dot{u}_j = \frac{u_{j+1} - 2u_j + u_{j-1}}{h^2} + \sigma\phi(X_j, t), \quad (2)$$

where an overdot denotes the derivative d/dt , and u_j is the value of the field $u(x, t)$ at the grid points X_j . However, the analysis of Section 3 recommends we use instead

$$\dot{u}_j \approx \frac{u_{j+1} - 2u_j + u_{j-1}}{h^2} + \sigma \left[\sqrt{\frac{5}{7}}\psi_j - \frac{1}{24}\sqrt{\frac{7}{5}}(\psi_{j+1} - 2\psi_j + \psi_{j-1}) + \sqrt{\frac{2}{7}}\hat{\psi}_j \right], \quad (3)$$

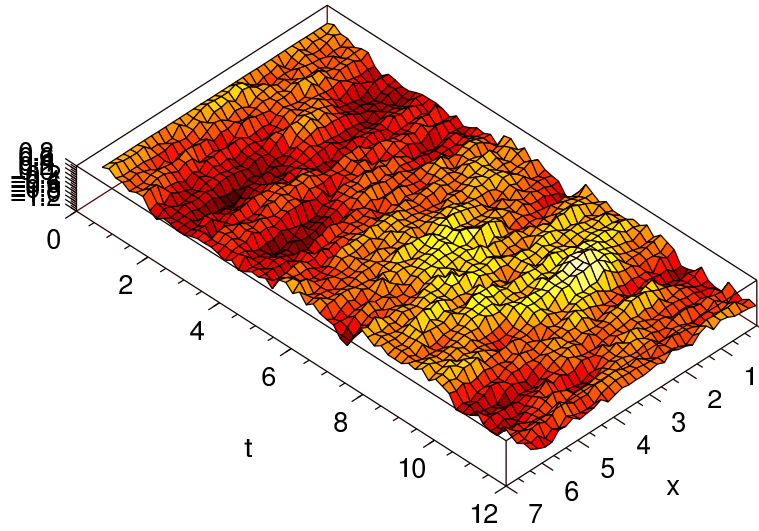


Figure 2: an example microscale simulation of one realisation of the stochastically forced diffusion SPDE, Burgers' SPDE (1) with nonlinearity $\alpha = 0$, and noise intensity $\sigma = 1$. This simulation uses (2) on a fine space-time mesh with $\Delta x = \pi/16$ and $\Delta t = 0.01$ but plotted every 19th time step.

see (27), for some noise processes ψ_j and $\hat{\psi}_j$. The rationale is that spatial diffusion on the subgrid microscale in between the grid points weakly correlates the noise that should be applied to each grid value. Thus the point sample $\phi_j(t) = \phi(X_j, t)$ of the noise $\phi(x, t)$ should be replaced by two components: a component $\hat{\psi}_j(t)$ which is uncorrelated across the grid points; and a component $\psi_j(t)$ which has an influence distributed over the evolution of three neighbouring grid values. Figure 4 confirms the veracity of the model SDE (3) as explained in Section 3.4. In order to find the interactions between noise and diffusion which are expressed in (3) we account explicitly for subgrid microscale physical processes.

Centre manifold theory has wonderful characteristics for creating low dimensional models of dynamical systems (see the book by Carr [8] for a good introduction). It addresses the evolution of a dynamical system in a neighbourhood of a marginally stable fixed point; based upon the linear dynamics the theory guarantees that an accurate low-dimensional description of the nonlinear dynamics may be deduced. The theory is a powerful tool for the modelling of complex dynamical systems [9, 10, 35, 40, 22, 48, e.g.]. I apply the stochastic centre manifold (SCM) theory of Boxler [5] to the discretisation of SPDEs such as Burgers' SPDE (1).

1.1 Divide space into discrete finite elements

The method of lines discretises a deterministic PDE in space \mathbf{x} and integrates in time as a set of ordinary differential equations; this method is sometimes called a semi-discrete scheme [20, 21, e.g.]. Similarly, we only discuss the spatial discretisation of SPDEs and treat the resulting set of stochastic ordinary differential equations, such as the SDE (3), as a continuous time, stochastic dynamical system.

Place the discretisation of the nonlinear SPDEs, such as Burgers' SPDE (1), within the purview of SCM theory by the following artifice. Let equi-spaced grid points at \mathbf{x}_j be a distance h apart. Then the j th element is notionally $|\mathbf{x} - \mathbf{X}_j| < h/2$. Form finite elements by introducing the artificial internal coupling conditions (ICCs)

$$\mathbf{u}_j(\mathbf{X}_{j\pm 1}, t) - \mathbf{u}_j(\mathbf{X}_j, t) = \gamma [\mathbf{u}_{j\pm 1}(\mathbf{X}_{j\pm 1}, t) - \mathbf{u}_j(\mathbf{X}_j, t)], \quad (4)$$

where $\mathbf{u}_j(\mathbf{x}, t)$ denotes the subgrid microscale field of the j th element. The coupling parameter γ controls the flow of information between adjacent elements: when $\gamma = 0$, adjacent elements are decoupled; whereas when $\gamma = 1$, the field in the j th element must extrapolate to the neighbouring elements' field at their grid point. These ICCs ensure discrete models are consistent with linear deterministic PDEs to high order as the element size $h \rightarrow 0$ [45]; all examples also show these ICCs produce high order consistency for the nonlinear dynamics but no proof yet exists.

Importantly, the methodology developed here applies to a wide variety of other SPDEs, not just Burgers' SPDE (1). Some representative examples in deterministic PDEs are: the approach models accurately the nonlinear dynamics of the fourth order Kuramoto–Sivashinsky equation [31, 33]; a web page analyses any reasonable second, fourth or sixth order PDE or set of three coupled PDEs entered by a browsing client [47]; and two dimensional advection diffusion along a channel is modelled by a one dimensional discrete shear dispersion [32]. Similar to these deterministic examples, the modelling of SPDEs only relies on the existence of a discrete centre-stable spectrum of the linear operator *on a finite element*. Consequently, the methodology developed here creates discretisations for an enormously wide range of SPDEs.

1.2 Model nonlinear stochastic dynamics

Via the analysis of Sections 4 and 5, a low order accurate discrete model SDE of the nonlinear dynamics of the stochastically forced Burgers' SPDE (1) is

$$\dot{\mathbf{u}}_j \approx \frac{1}{h^2} \left(1 + \frac{1}{12} \alpha^2 h^2 \mathbf{u}_j^2 \right) (\mathbf{u}_{j+1} - 2\mathbf{u}_j + \mathbf{u}_{j-1}) - \alpha \frac{1}{2h} \mathbf{u}_j (\mathbf{u}_{j+1} - \mathbf{u}_{j-1})$$

$$+ \sigma \left[\phi_{j,0} - \alpha \frac{2h}{\pi^2} \phi_{j,1} u_j - \alpha^2 \frac{8h^2}{3\pi^4} \phi_{j,2} u_j^2 \right] + .01643 \alpha^2 h^2 \sigma^2 u_j, \quad (5)$$

when the subgrid microscale noise within each element is truncated to the first three Fourier modes:

$$\phi(x, t) = \phi_{j,0}(t) + \phi_{j,1}(t) \sin[\pi(x - X_j)/h] + \phi_{j,2}(t) \cos[2\pi(x - X_j)/h].$$

The first line of the discretisation (5) is the so-called holistic discretisation for the deterministic Burgers' equation. This deterministic discretisation has good properties on finite sized elements [43]; in particular, the nonlinearly enhanced diffusion promotes stability of the scheme for non-small field u . The second line of the discretisation (5) approximates some of the influences of the forcing noise: observe that the nonlinearity in the subgrid microscale dynamics of Burgers' equation transforms the additive noise forcing of the SPDE (1) into multiplicative noise components in the discretisation. Simple modelling schemes miss such multiplicative noise terms because they do not resolve the subgrid microscale processes.

Stochastic forcing generates high wavenumber, steep variations, in spatial structures, see Figure 1. Through a form of stochastic resonance a reasonably accurate resolution of the life-time of these modes may be important on the large scale dynamics. For example, the discrete model SDE (5) includes a term proportional to $\sigma^2 u_j$ that arises from the self-interactions of noise, as flagged by the σ^2 factor and discussed in Section 5.3; here this term demonstrates that subgrid microscale noise interactions may contribute to destabilise the equilibrium $u = 0$. Herein the term “stochastic resonance” includes phenomena where stochastic fluctuations interact with each other and themselves through nonlinearity in the dynamical system to generate not only long time drifts but also potentially to change stability [30, 5, 18, 49, 57, e.g.]. Consequently, discrete model SDEs, such as (5) and (3), which must use on large space-time grids for efficiency, must also account for subgrid microscale dynamics in their closure in order to resolve the significant subtle interactions that take place on the subgrid microscale.

Stable implicit integration schemes do not resolve subgrid microscale fluctuations. For example, recall that the well established Crank–Nicholson scheme for spatio-temporal dynamics is based upon the stability of the implicit scheme

$$\frac{u_{t+\Delta t} - u_t}{\Delta t} = -\beta \frac{u_{t+\Delta t} + u_t}{2} \quad \text{for the ODE} \quad \dot{u} = -\beta u.$$

The solution is indeed stable,

$$u(t) = u(0) \left(\frac{1 - \beta \Delta t / 2}{1 + \beta \Delta t / 2} \right)^{t/\Delta t},$$

and accurate for small $\beta\Delta t$. Thus in general such schemes may well preserve noise characteristics, such as drift and volatility, of the evolution of *slow* macroscopic modes which have small β . However, the dynamics of microscale modes, with large $\beta\Delta t$, is badly misrepresented by such a scheme when employing a macroscopic time step of relatively large Δt ; for example, any exponential decay of microscale modes is badly simulated by near oscillations, approximately $(-1)^{t/\Delta t}$. Thus subtle subgrid microscale effects quadratic in noise intensity are irretrievably misrepresented by Crank–Nicholson like schemes. In contrast, the methodology proposed here provides a systematic method for macroscale closure of the microscale noise.

Stochastic centre manifold theory supports the large time macroscopic modelling of detailed stochastic microscopic dynamics. For example, Knobloch & Wiesenfeld [30] and Boxler [5, 6] explicitly used SCM theory to support the modelling of SDEs and SPDEs. Boxler [5] proves that “stochastic center manifolds, share all the nice properties of their deterministic counterparts”. Many, such as Berglund & Gentz [3], Blömker, Hairer & Pavliotis [4] and Kabanov & Pergamenschikov [28], use the same separation of time scales that underlies SCM theory to form and support low dimensional, long time models of SDEs and SPDEs that have both fast and slow modes. Similarly, Bensoussan & Flandoli [2] proved the existence and relevance of finite dimensional stochastic inertial manifolds for a wide class of stochastic systems in a Hilbert space. Centre manifold theory also supports the discretisation on finite sized grids of deterministic partial differential equations [43, 45, 31, 44, 46, 32]. By merging these two applications of centre manifold theory we model SPDEs with sound theoretical support, as described in Section 2. Coupling many finite elements together forms macroscale discrete models of SPDEs such as (3) and (5). The fiendish complication is to account for noise and its dynamics which are distributed independently across space as well as time, both within a finite element and between neighbouring finite elements. Computer algebra [50] handles the details of the nonlinear subgrid dynamics and the inter-element interactions.

We discuss the forcing $\phi(\mathbf{x}, t)$ as a white noise, that is, $\phi(\mathbf{x}, t)$ is delta correlated in both space and time. However, computational limitations often require the truncation to a few Fourier modes as in (5). However, most of the analysis and models in Sections 2–4 also hold for deterministic forcing $\phi(\mathbf{x}, t)$. Correlated noise ϕ could be handled with the same methodology by introducing auxiliary SPDEs such as

$$\frac{\partial \phi}{\partial t} = -\mathcal{G} \star \phi + \xi(\mathbf{x}, t).$$

For some white space-time noise ξ and convolution kernel $\mathcal{G}(\mathbf{x})$ the stochastic

effects in an SPDE would have spatial correlations with power spectrum $\propto 1/\tilde{\mathcal{G}}(\mathbf{k})$ for Fourier transform $\tilde{\mathcal{G}}$ of the kernel $\mathcal{G}(\mathbf{x})$. Consequently, this approach encompasses quite general noise processes.

Interpret all noise processes and all stochastic differential equations in the Stratonovich sense so that the rules of traditional calculus apply. Thus the direct application of this modelling is to physical systems where the Stratonovich interpretation is the norm. This use of the Stratonovich calculus is thus most appropriate for the main application areas of physicists and engineers.

2 Stochastic centre manifold theory underpins modelling

I detail one way to place the spatial discretisation of SPDEs within the purview of stochastic centre manifold (SCM) theory. Then, subject to some conditions, extant theory assures us of the existence and relevance of discrete models of the general SPDE

$$\frac{\partial \mathbf{u}}{\partial t} = \mathcal{L}\mathbf{u} + \alpha f(\mathbf{u}) + \sigma \phi(\mathbf{u}, \mathbf{x}, t) \quad (6)$$

where \mathcal{L} is a dissipative linear operator, $f(\mathbf{u})$ gives smooth, deterministic, linear and nonlinear perturbations, and ϕ gives the stochastic effects in the SPDE. The stochastic, forced, Burgers' equation (1) serves as a definite example of the broad class (6) of nonlinear, dissipative SPDEs for which the approach is applicable.

We *base* the discrete modelling upon the dynamics when: firstly, the noise is absent, $\sigma = 0$; secondly, each element is decoupled from its neighbours, $\gamma = 0$; and lastly, the nonlinearity is negligible, $\alpha = 0$. When $\sigma = \gamma = \alpha = 0$ the dynamics of the SPDE (6) with coupling conditions (4) reduce to that of linear dissipation within each element insulated from its neighbours:

$$\frac{\partial \mathbf{u}}{\partial t} = \mathcal{L}\mathbf{u} \quad \text{such that} \quad \pm h \frac{\partial \mathbf{u}}{\partial x} = 0 \text{ at } x = X_j \pm \frac{1}{2}h; \quad (7)$$

for example, Burgers' SPDE (1) linearises to the diffusion equation $\mathbf{u}_t = \mathbf{u}_{xx}$. The discrete coupling conditions (4) are most convenient for the construction of the discrete model. However, as reflected in the coupling conditions in (7), theory is most conveniently applied using the following coupling conditions which are equivalent to (4):

$$\pm h \frac{\partial \mathbf{u}_j}{\partial x} \Big|_{x=X_j \pm h/2} = \gamma \left[\mathcal{A}\mathbf{u}_{j \pm 1} \Big|_{x=X_{j \pm 1}} - \mathcal{A}\mathbf{u}_j \Big|_{x=X_j} \right], \quad (8)$$

where the near identity operator

$$\mathcal{A} = \frac{\pm h \partial_x}{\exp(\pm h \partial_x) - 1} = 1 \mp \frac{1}{2} \partial_x + \frac{1}{12} \partial_x^2 - \frac{1}{720} \partial_x^4 + \frac{1}{30240} \partial_x^6 + \mathcal{O}(\partial_x^8).$$

All discussions of theoretical support for the discretisation use the element coupling conditions (8) instead of the computationally convenient (4).

The theory also needs a definite domain. All discussions of theoretical support use a domain in space coordinate x of some length L . The boundary conditions are then that the field $u(x, t)$ is to be L periodic in x : that is, $u(x + L, t) = u(x, t)$. Equivalently, consider the SPDE (6) in the interior of a domain large enough so the physical boundaries are far enough away to be immaterial. The crucial aspect is that the analysis throughout assumes space and time are statistically homogeneous so that the resultant discretisations are statistically homogeneous as seen in (3) and (5). Returning to the periodic domain, divide the domain into M elements of equal and finite length $h = L/M$. The grid point $x = X_j$ is the mid-point of the j th element.

The base problem (7) has dissipative dynamics on each of the M elements. *Assume the spectrum $\{0, -\beta_1, -\beta_2, \dots\}$ of the dissipative operator \mathcal{L} is discrete with negative real parts: $0 > \Re(-\beta_1) > \Re(-\beta_2) > \dots$.* For example, the base problem of Burgers' SPDE (1) is spatial diffusion which within each element has spectrum given by the negative of the decay rates

$$\beta_k = \frac{\pi^2 k^2}{h^2}, \quad k = 0, 1, 2, \dots; \quad (9)$$

the corresponding orthogonal eigenfunctions $v_k(x - X_j)$ are the Fourier modes

$$v_k(x - X_j) = \text{csn } k\theta = \begin{cases} \cos k\theta, & \text{for even } k, \\ \sin k\theta, & \text{for odd } k, \end{cases} \quad (10)$$

where the integer k is the subgrid microscale wavenumber, and $\theta = \pi(x - X_j)/h$ measures subgrid position relative to the grid point within each element—the j th element lies between $\theta = \pm\pi/2$. The $k = 0$ mode, $u \propto v_0$ in each element (usually constant), is linearly neutral as its decay rate $\beta_0 = 0$. Thus, in the linearised dynamics, subgrid structures within each element exponentially quickly decay to v_0 .

Decompose the noise within each element as a linear combination of the eigenfunctions v_k of the linear dissipation \mathcal{L} . Analogous to Example 5.2.2 of Da Prato & Zabczyk [14, see also p.259], for the example Burgers' SPDE (1) we use the Fourier modes (10):

$$\phi(x, t) = \sum_{k=0}^{\infty} \phi_{j,k}(t) v_k(x - X_j) = \sum_{k=0}^{\infty} \phi_{j,k}(t) \text{csn } k\theta, \quad \text{for } |x - X_j| < h/2, \quad (11)$$

where $\phi_{j,k}$ denotes the noise process of the k th wavenumber in the j th element. Assume the set of noise processes $\{\phi_{j,k}\}$ are independent. Typically, the components of the forcing noise (11) with wavenumber $k \geq 1$ are orthogonal to the neutral basic mode v_0 in each element. Consequently, simple numerical methods, such as Galerkin projection onto the coarsest mode v_0 , would ignore the “high wavenumber” modes v_k , $k \geq 1$, of the noise (11) and hence completely miss subtle but important subgrid and inter-element interactions such as those seen in the models (3) and (5). In contrast, the systematic nature of SCM theory accounts for subgrid microscale interactions as a power series in the noise amplitude σ , the inter-element coupling γ and the nonlinearity α .

A stochastic slow manifold exists The nonlinear forced SPDE (6) with inter-element coupling conditions (8) linearises to the dissipative PDE (7). To account for parameter variations, adjoin the three trivial DES $d\epsilon/dt = 0$, where $\epsilon = (\sigma, \gamma, \alpha)$. In the extended state space (u, ϵ) , the linearised PDE has $M + 3$ eigenvalues of zero and all other eigenvalues have negative real part $\leq -\Re\beta_1$: this upper bound is $-\pi^2/h^2$ for the example of Burgers’ SPDE (1). Thus the linear dissipative PDE (7) has an $M + 3$ dimensional slow subspace: called ‘slow’ because all the corresponding eigenvalues are precisely zero. Consequently, SCM assures us a corresponding $M + 3$ dimensional stochastic slow manifold (SSM) exists.¹

Lemma 1 *For Lipschitz nonlinearities $f(u)$ and in some finite neighbourhood of $(u, \epsilon) = (0, 0)$ there exists an $M + 3$ dimensional SSM for the SPDE (6) in which the field in the j th element is $u = u_j(U(t), x, t, \epsilon)$ where the j th component U_j of vector U measures the amplitude of the neutral mode $v_0(x - X_j)$ in the j th element, and where the amplitudes U_j evolve according to $\dot{U}_j = g_j(U, t, \epsilon)$ for some function g_j , but provided*

- *either the nonlinear SPDE (6) is effectively finite dimensional [5, Theorems 5.1 and 6.1] (that is, there exists a wavenumber K such that modes v_k for $k \geq K$ do not affect through f or ϕ the dynamics for modes with $0 \leq k < K$);*
- *or the noise in the SPDE (6) is multiplicatively linear in u , $\phi = u\psi(x, t)$, [58, Theorem A].*

¹Of the dimensions of the SSM, M dimensions arise from the one neutral mode v_0 within each of the M elements, and three dimensions arise from the dependence upon the three parameters $\epsilon = (\sigma, \gamma, \alpha)$.

Similarly, Blömker et al. [4, Theorem 1.2] rigorously proved the existence and relevance of a stochastic Ginzburg–Landau model to the ‘infinite dimensional’ stochastic forced Swift–Hohenberg PDE; further, Caraballo, Langa & Robinson [7] and Duan, Lu & Schmalfuss [19] analysed the existence of invariant manifolds for a wide class of ‘infinite dimensional’ reaction-diffusion SPDEs with linearly multiplicative noise; they built on earlier work by Bensoussan & Flandoli [2] proving the existence and relevance of inertial manifolds of SPDEs in a Hilbert space. Wang & Duan [58] also proved the existence of attractive slow manifolds for a wide class of SPDEs but again only with linearly multiplicative noise.

Unfortunately, many interesting physical problems do not have Lipschitz nonlinearity; for example, the nonlinear advection in Burgers’ SPDE (1) involves the unbounded operator $\partial/\partial x$. I expect future theoretical developments should rigorously support this approach. However, in the interim, let us proceed via a type of shadowing argument [51]. The rapid dissipation of high wavenumber modes in applications such as Burgers’ SPDE (1) ensures that the dynamics is close to finite dimensional. For example, I showed that resolving just ten subgrid modes in a modified Burgers’ SPDE (1) was sufficient to give the coefficients of the evolution on a SSM correct to five digits [51, §4]. By modifying the spatial derivatives in (1) to have a high wavenumber cutoff, as done in Section 4, the dynamics of Burgers’ SPDE (1) is effectively that of a Lipschitz, finite dimensional system. The theorems of Boxler [5] then rigorously apply.

Such a cutoff is used in rigorous theory. For example, Da Prato & Zabczyk [14, p.265] define a so-called ‘mollifier’ $M_R(x)$ which is identically x for $\|x\| < R$ and which is zero for $\|x\| > 2R$. For Burgers’ SPDE (1) with nonlinearity modified by the mollifier, Da Prato & Zabczyk prove existence and uniqueness of solutions. In essence, the above ‘wavenumber cutoff’ performs the same regularising role as their mollifier.

The stochastic slow manifold model captures the dynamics The second key property of SCMs is that the evolution on the SSM does capture the long term dynamics of the original SPDE (6). In this context, the discrete model on the SSM describes all the dynamics of the SPDE (6) apart from exponentially decaying transients. For example, all solutions of Burgers’ SPDE (1) close enough to the origin are exponentially quickly described by the discretisation (5). This amazing theoretical support for the model holds at finite element size h .

Boxler’s Relevance Theorem 7.1(i) [5] and Wang & Duan’s Theorem A [58] are rephrased in the following lemma (see also Theorem 2.3(iii) by Bensoussan

& Flandolfi [2]).

Lemma 2 (Relevance) *For the conditions of Lemma 1, there is a neighbourhood \mathbf{N} of the origin such that for each solution $\mathbf{u}(\mathbf{x}, \mathbf{t})$ of the SPDE (6) remaining in the neighbourhood \mathbf{N} , with α , γ and σ constant, there exists a solution $\mathbf{U}(\mathbf{t})$ on the SSM such that $\|\mathbf{u} - \mathbf{u}_j(\mathbf{U}, \mathbf{x}, \mathbf{t}, \epsilon)\| \rightarrow 0$ as $\mathbf{t} \rightarrow \infty$ almost surely.*

Boxler also assures us that the rate of decay to the SSM is of the same magnitude as the decay of the gravest subgrid microscale mode [5, Theorem 7.1(i)], here $\exp(-\beta_1 \mathbf{t})$. Thus, for example, on times significantly larger than a cross element diffusion time h^2/π^2 , the exponential transients decay and the SSM model (5) describes the dynamics of Burgers' SPDE (1).

Subtleties in this theorem mislead some researchers even when modelling deterministic systems. For example, Givon et al. [24] discuss finite dimensional deterministic systems which linearly separate into slow modes $\mathbf{x}(\mathbf{t})$ and fast, stable modes $\mathbf{y}(\mathbf{t})$. They identify the existence of a slow invariant manifold $\mathbf{y} = \boldsymbol{\eta}(\mathbf{x})$ and the low dimensional evolution on the manifold in the form $\dot{\mathbf{X}} = \mathbf{L}_1 \mathbf{X} + \mathbf{f}(\mathbf{X}, \boldsymbol{\eta}(\mathbf{X}))$. However, they *assume* [24, p.R67, bottom] that the initial condition for the evolution on the slow manifold is simply $\mathbf{X}(0) = \mathbf{x}(0)$, and then later, just after their (4.5), place undue restrictions on the possible initial conditions. However, the source of the problem is that this initial value for $\mathbf{X}(0)$ is generally inaccurate. Cox & Roberts [13, 41] identified that a specified initial condition $(\mathbf{x}(0), \mathbf{y}(0))$ has to be projected onto a deterministic slow manifold *along isochrons* to an initial condition $\mathbf{X}(0) \neq \mathbf{x}(0)$; physicists sometimes call this difference between $\mathbf{x}(0)$ and $\mathbf{X}(0)$ the 'initial slip' [25, e.g.]. The correct initial condition for discretisations of deterministic PDEs is similarly some nontrivial projection of a specified initial condition [44]. Only then does the model solution track the full solution exponentially quickly as assured by the Relevance Theorems. For stochastic systems, similar nontrivial projection of specific initial conditions onto the SSM may be realised via stochastic normal forms [1, e.g.].

However, there are two significant caveats to our application of Lemma 2 to discretising SPDEs. Firstly, although the asymptotic series we do construct are global in the grid value amplitudes \mathbf{U}_j , they are local in the parameters $\epsilon = (\sigma, \gamma, \alpha)$. Thus the rigorous theoretical support only applies in some finite neighbourhood of $\epsilon = \mathbf{0}$. At this stage we have little information on the size of that neighbourhood. In particular, we need to evaluate the model when $\gamma = 1$ to recover a discrete model for fully coupled elements; thus we desire $\gamma = 1$ to be in the finite neighbourhood of validity. This has been demonstrated for the deterministic Burgers' equation [43], but not yet for the stochastic case. Secondly, we cannot construct the SSM and the

evolution thereon exactly; it is difficult enough constructing asymptotic approximations such as the low order accuracy models (3) and (5). Thus the models we develop and discuss have an error due to the finite truncation of the asymptotic series in the small parameters ϵ .

For example, the truncation in powers of the coupling parameter γ controls the width of the computational stencil for the discrete models. Due to the form of the coupling conditions (4) or (8), nearest neighbour elements interactions are flagged by terms in γ^1 , whereas interactions with next to nearest neighbouring elements occur as γ^2 terms, and so on for higher powers. The low accuracy models (3) and (5) are constructed with error $\mathcal{O}(\gamma^2)$ and so summarise the interactions between the dynamics in an element and those of its two immediate neighbours.

In a nonlinear system the noise processes interact with each other and themselves. But dealing with nonlinear stochastic dynamics is gruesomely complicated and so Section 3 first introduces some of the techniques in the considerably simpler example of stochastically forced diffusion.

3 Construct a memoryless normal form of diffusion

This section explores the discretisation of the non-dimensional stochastically forced diffusion equation

$$\frac{\partial u}{\partial t} = \frac{\partial^2 u}{\partial x^2} + \sigma \phi(x, t); \quad (12)$$

Figure 2 shows a simulation of one realisation. This stochastically forced diffusion is the special case of the general SPDE (6) if the linear operator $\mathcal{L} = \partial_{xx}$ when the nonlinearity parameter $\alpha = 0$; Burgers' SPDE (1) for example. We explore how to construct a SSM model of the discretised dynamics. Because the dynamics of diffusion are linear, the SSM methodology is significantly easier to explore in comparison to that needed for nonlinear SPDEs.

In iteratively constructing the SSM, §3.1, we encounter convolution integrals over the immediate past of the noise, §3.2. Such fast time ‘memory’ convolutions must be removed from the dynamics of the discretisation, §3.3 Givon et al. [24, p.R59] similarly comment “Memory. An important aim of any such algorithm is to choose \mathbf{P} [the SSM] in such a way that the dynamics in \mathbf{X} [the grid values \mathbf{U}] is memoryless.” We simplify the discrete model tremendously by removing such ‘memory’ convolutions as originally developed for SDEs by Couillet, Elphick & Tirapegui [12], Sri Namachchivaya & Lin [55], and Roberts & Chao [11, 49]. The results are discrete models, such

as (3), where the noise is correlated across neighbouring elements, §3.4–3.5, despite the originally uncorrelated noise in the SPDE (12).

3.1 Iteration converges to the asymptotic series

As discussed in Section 2, SCM theory supports discretisations of the SPDE (6). The construction theorem only depends upon finding a model for which the residuals of the governing equations are of some specified order of smallness: for example, Boxler [5, Theorem 8.1] assures us that if we satisfy the diffusion SPDE (12) to some residual $\mathcal{O}(\epsilon^q)$, then the SSM and the evolution thereon have the same order of error, namely $\mathcal{O}(\epsilon^q)$. Recall that noise intensity σ and inter-element coupling γ are the small parameters in the asymptotic series forming the SSM discrete model of the diffusion. Because the critical aspect of constructing the SSM model is simply the ultimate order of the residual of the SPDE (6), the specific details of the computation are not recorded here. Instead computer algebra performs all the details [50]. This section reports on critical steps in the method as displayed in its application to the diffusion SPDE (12).

Consider the task of iteratively constructing a SSM model for the SPDE (12) [42]. We seek solutions such that in the j th element the stochastic field $\mathbf{u} = \mathbf{u}_j(\mathbf{U}, \mathbf{x}, \mathbf{t}, \boldsymbol{\epsilon}) = \mathbf{U}_j + \dots$ such that the vector of amplitudes \mathbf{U} evolve according to some specific SDE $\dot{\mathbf{U}}_j = \mathbf{g}_j(\mathbf{U}, \mathbf{t}, \boldsymbol{\epsilon})$, such as (3). The steps in the construction proceed iteratively. Suppose that at some stage we have some asymptotic approximation to the model, then the next iteration is to seek small corrections, denoted \mathbf{u}'_j and \mathbf{g}'_j , to improve the asymptotic approximation. As the iterations proceed, the small corrections \mathbf{u}'_j and \mathbf{g}'_j get systematically smaller, that is, of higher order in the small parameters $\boldsymbol{\epsilon}$ of the asymptotic series. As explained in [42], substitute $\mathbf{u} = \mathbf{u}_j + \mathbf{u}'_j$ and $\dot{\mathbf{U}}_j = \mathbf{g}_j + \mathbf{g}'_j$ into the SPDE (12), then linearise the problem for \mathbf{u}'_j and \mathbf{g}'_j by dropping products of small corrections. Thus obtain that the corrections should satisfy

$$\frac{\partial \mathbf{u}'_j}{\partial \mathbf{t}} - \mathcal{L} \mathbf{u}'_j + \mathbf{g}'_j = \text{residual}_{(12)}, \quad (13)$$

where $\mathcal{L} = \partial_{xx}$ for the diffusion SDE (12). Here the “residual” is the residual of the SPDE (12) evaluated for the currently known asymptotic approximation. Further, the inter-element coupling conditions (4) provide boundary conditions for \mathbf{u}'_j : substitute $\mathbf{u} = \mathbf{u}_j + \mathbf{u}'_j$ into (4); linearise by dropping small $\gamma \mathbf{u}'_j$ terms; and obtain that the correction PDE (13) needs to be solved with the coupling conditions

$$\mathbf{u}'_j(\mathbf{X}_{j\pm 1}, \mathbf{t}) - \mathbf{u}'_j(\mathbf{X}_j, \mathbf{t}) + \text{residual}_{(4)} = 0. \quad (14)$$

For example, suppose at some stage we had found the deterministic part of the model in the j th element was that of classic Lagrangian interpolation

$$\begin{aligned} u_j(x, t) &= U_j + \gamma \left[\frac{1}{2}(\theta/\pi)^2 \delta^2 + (\theta/\pi) \mu \delta \right] U_j + \mathcal{O}(\sigma + \gamma^2) \\ \text{such that } \dot{U}_j &= \frac{\gamma}{h^2} \delta^2 U_j + \mathcal{O}(\sigma + \gamma^2), \end{aligned} \quad (15)$$

where throughout this article the discrete difference and mean operators [38, p.65, e.g.] reduce the algebraic length of expressions, respectively

$$\delta U_j = U_{j+1/2} - U_{j-1/2} \quad \text{and} \quad \mu U_j = \frac{1}{2} (U_{j+1/2} + U_{j-1/2}).$$

Then using (15) in the next iteration, the diffusion SDE's

$$\text{residual}_{(12)} = -\frac{\gamma^2}{h^2} \left[(\theta/\pi) \mu \delta^3 + \frac{1}{2}(\theta/\pi)^2 \delta^4 \right] U_j + \sigma \sum_{k=0}^{\infty} \phi_{j,k}(t) \text{csn } k\theta, \quad (16)$$

whereas the coupling conditions have

$$\text{residual}_{(4)} = 0. \quad (17)$$

3.2 Corrections from a simple residual

Now explore how to solve (13–14) for corrections given some residual such as (16–17). The terms in the residual split into two categories, as is standard in singular perturbations:

- Each subgrid component in $v_k(x - X_j)$ for $k \geq 1$ causes no great difficulty; we include a corresponding component in the correction u'_j to the field in proportion to v_k —when the coefficient in the residual is time dependent, say $\phi_{j,k}(t)v_k$, the component in the correction u'_j is $\mathcal{Z}_k \phi_{j,k}(t)v_k$ in which the operator \mathcal{Z}_k denotes convolution over past history with $\exp[-\beta_k t]$, namely

$$\mathcal{Z}_k \phi = \exp[-\beta_k t] \star \phi(t) = \int_{-\infty}^t \exp[-\beta_k(t - \tau)] \phi(\tau) d\tau; \quad (18)$$

recall that β_k is the (positive) decay rate (9) of the k th mode within each element; $\beta_k = k^2 \pi^2 / h^2$ in the case of diffusion (12) or Burgers' SPDE (1). Da Prato & Zabczyk [14, §5.2.1] discuss the existence and continuity of such stochastic convolutions.

- But the correction \mathbf{g}'_j to the evolution gets a contribution from any component in the residual of the neutral mode \mathbf{v}_0 , that is, constant across the element. For example, the component $\sigma\phi_{j,0}(\mathbf{t})$ in the residual (16) forces the correction $\mathbf{g}'_j = \sigma\phi_{j,0}$ as no uniformly bounded component in \mathbf{u}'_j can match a constant component of the residual—this is the standard solvability condition for singular perturbations.

For example, with residuals (16–17) the corresponding corrections \mathbf{g}'_j and \mathbf{u}'_j improve the SSM (15) to

$$\begin{aligned} \mathbf{u}_j(\mathbf{x}, \mathbf{t}) = & \mathbf{U}_j + \gamma \left[\frac{1}{2}(\theta/\pi)^2 \delta^2 + (\theta/\pi)\mu\delta \right] \mathbf{U}_j \\ & + \gamma^2 \left[\frac{1}{6}((\theta/\pi)^3 - (\theta/\pi))\mu\delta^3 + \frac{1}{24}((\theta/\pi)^4 - (\theta/\pi)^2)\delta^4 \right] \mathbf{U}_j \\ & + \sigma \sum_{k=1}^{\infty} \mathcal{Z}_k \phi_{j,k} \cos k\theta + \mathcal{O}(\sigma^{3/2} + \gamma^3), \end{aligned} \quad (19)$$

$$\dot{\mathbf{U}}_j = \frac{\gamma}{h^2} \delta^2 \mathbf{U}_j - \frac{\gamma^2}{12h^2} \delta^4 \mathbf{U}_j + \sigma\phi_{j,0} + \mathcal{O}(\sigma^{3/2} + \gamma^3), \quad (20)$$

The γ^2 corrections in (20) modify the deterministic terms of the model (15) to (when $\gamma = 1$) classic finite difference expressions of fourth order consistency as element size $h \rightarrow 0$; the noise induced σ terms in (20) are the straight-forward forcing of the model dynamics. It is the next iteration that begins to account for interesting subgrid microscale stochastic processes within the finite sized elements.

Let the amplitude be flexible Observe that the SSM field (19) evaluated at the grid points $\mathbf{x} = \mathbf{X}_j$ is no longer the amplitude \mathbf{U}_j . Instead, with the correction leading to (19) the grid value $\mathbf{u}(\mathbf{X}_j, \mathbf{t}) = \mathbf{U}_j + \sigma \sum_{k=2, \text{even}}^{\infty} \mathcal{Z}_k \phi_{j,k}$. Insisting that the evolution $\dot{\mathbf{U}}_j = \mathbf{g}'_j$ does not have any memory convolutions implies we cannot also require the amplitudes \mathbf{U}_j to be the grid values $\mathbf{u}(\mathbf{X}_j, \mathbf{t})$. We must abandon absolute control over the meaning of the amplitudes when modelling non-autonomous dynamics. This holds for both deterministic and stochastic systems. In the geometry of state space, removing memory convolutions from the evolution *implicitly* requires that the amplitudes be constant along the so-called isochrons in the neighbourhood of the SSM [13].

3.3 Some convolutions need to be separated

A more delicate issue arises in subsequent corrections. Integration by parts separates noise convolutions into integrable and non-integrable components.

As usual, I discuss general issues via the example of the stochastically forced diffusion (12). The next iteration uses (19), whence the coupling conditions have

$$\text{residual}_{(4)} = \gamma\sigma \sum_{k=2,\text{even}}^{\infty} [\mathcal{Z}_k \phi_{j,k} - \mathcal{Z}_k \phi_{j\pm 1,k}] + \mathcal{O}(\sigma^3 + \gamma^3).$$

Satisfy the coupling conditions (14) with the above $\text{residual}_{(4)}$ by incorporating into the approximate field (19), the following correction \mathbf{u}'_j (quadratic across the element)

$$+\gamma\sigma \left[(\theta/\pi)\mu\delta + \frac{1}{2}(\theta/\pi)^2\delta^2 \right] \sum_{k=2,\text{even}}^{\infty} \mathcal{Z}_k \phi_{j,k}.$$

Then using the model SDE (20), and the above added to the right-hand side of the SSM (19), the diffusion SPDE (12) has

$$\begin{aligned} \text{residual}_{(12)} = & \gamma\sigma\delta^2 \sum_{k=2,\text{even}}^{\infty} \left(\frac{1}{h^2} + \frac{\beta_k}{24} \right) \mathcal{Z}_k \phi_{j,k} - \gamma\sigma \frac{1}{24} \delta^2 \sum_{k=0,\text{even}}^{\infty} \phi_{j,k} \\ & - \gamma\sigma \frac{4}{\pi^2} \sum_{k=1,\text{odd}}^{\infty} \frac{(-1)^{\frac{k-1}{2}}}{k^2} \sin k\theta \mu\delta \left[\sum_{\ell=0,\text{even}}^{\infty} \phi_{j,\ell} - \sum_{\ell=2,\text{even}}^{\infty} \beta_{\ell} \mathcal{Z}_{\ell} \phi_{j,\ell} \right] \\ & - \gamma\sigma \frac{2}{\pi^2} \sum_{k=2,\text{even}}^{\infty} \frac{(-1)^{k/2}}{k^2} \cos k\theta \delta^2 \left[\sum_{\ell=0,\text{even}}^{\infty} \phi_{j,\ell} - \sum_{\ell=2,\text{even}}^{\infty} \beta_{\ell} \mathcal{Z}_{\ell} \phi_{j,\ell} \right] \\ & + \mathcal{O}(\sigma^3 + \gamma^3), \end{aligned} \quad (21)$$

with coupling condition $\text{residual}_{(4)} = \mathcal{O}(\sigma^3 + \gamma^3)$. The terms in the residual (21) involve the interaction of noise terms with the inter-element coupling, indicated by a $\sigma\gamma$ factor. The generic features in this residual are the sums over the microscale subgrid structures $\mathbf{v}_k = \text{csn } k\theta$, $k \geq 1$, and, in the first line, that the coarsest mode, $\mathbf{v}_0 = 1$, is forced by memory convolutions of the noise components.

We proceed to find the correction that the residual (21) forces through solving (13) which identifies how such a forcing affects the subgrid diffusion and time evolution. The components in the microscale subgrid structure $\mathbf{v}_k = \text{csn } k\theta$ above are not an issue; they just induce a corresponding component in the correction \mathbf{u}'_j via a further convolution \mathcal{Z}_k . The components constant across the element, in the first line above, are the delicate issue:

- we cannot match them by corrections \mathbf{u}'_j as then \mathbf{u}'_j would contain integrals in time of the noise processes which in general grow secularly like \sqrt{t} ;

- neither can they be matched by corrections to the evolution \mathbf{g}'_j as then incongruous fast-time convolution integrals would appear in the model of the long term dynamics.

The appropriate alternative [12, 55, 11, 49] recognises that part of these components can be integrated in time: for any $\phi(t)$, $\frac{d}{dt}\mathcal{Z}_k\phi = -\beta_k\mathcal{Z}_k\phi + \phi$, from the convolution definition (18), thus

$$\mathcal{Z}_k\phi = \frac{1}{\beta_k} \left[-\frac{d}{dt}\mathcal{Z}_k\phi + \phi \right], \quad (22)$$

and so separate such a convolution in the residual, when multiplied by the neutral mode of a constant across the element, into:

- the first part, $-\frac{d}{dt}\mathcal{Z}_k\phi/\beta_k$, which is integrated into the next update \mathbf{u}'_j for the subgrid field;
- and the second part, ϕ/β_k , which updates \mathbf{g}'_j without introducing a fast-time memory convolution into the evolution.

This separation applies throughout the analysis of effects linear in the noise. When the residual component has many convolutions, then apply this separation recursively.

For the example diffusion SPDE (12), the terms in the first line of the example residual (21) force terms

$$-\gamma\sigma\delta^2 \sum_{k=2,\text{even}}^{\infty} \left(\frac{1}{\pi^2 k^2} + \frac{1}{24} \right) \mathcal{Z}_k\phi_{j,k}$$

into the subgrid SSM field making it now

$$\begin{aligned} \mathbf{u}_j(\mathbf{x}, t) = & \mathbf{U}_j + \gamma \left[\frac{1}{2}(\theta/\pi)^2\delta^2 + (\theta/\pi)\mu\delta \right] \mathbf{U}_j \\ & + \gamma^2 \left[\frac{1}{6}((\theta/\pi)^3 - (\theta/\pi))\mu\delta^3 + \frac{1}{24}((\theta/\pi)^4 - (\theta/\pi)^2)\delta^4 \right] \\ & + \sigma \sum_{k=1}^{\infty} \mathcal{Z}_k\phi_{j,k} \cos k\theta \\ & - \gamma\sigma\frac{4}{\pi^2} \sum_{k=1,\text{odd}}^{\infty} \frac{(-1)^{\frac{k-1}{2}}}{k^2} \sin k\theta \mu\delta \left[\sum_{\ell=0,\text{even}}^{\infty} \mathcal{Z}_k\phi_{j,\ell} - \sum_{\ell=2,\text{even}}^{\infty} \beta_{\ell}\mathcal{Z}_{k,\ell}\phi_{j,\ell} \right] \\ & - \gamma\sigma\frac{2}{\pi^2} \sum_{k=2,\text{even}}^{\infty} \frac{(-1)^{k/2}}{k^2} \cos k\theta \delta^2 \left[\sum_{\ell=0,\text{even}}^{\infty} \mathcal{Z}_k\phi_{j,\ell} - \sum_{\ell=2,\text{even}}^{\infty} \beta_{\ell}\mathcal{Z}_{k,\ell}\phi_{j,\ell} \right] \\ & - \gamma\sigma\delta^2 \sum_{k=2,\text{even}}^{\infty} \left(\frac{1}{\pi^2 k^2} + \frac{1}{24} \right) \mathcal{Z}_k\phi_{j,k} + \mathcal{O}(\sigma^3 + \gamma^3), \end{aligned} \quad (23)$$

where $\mathcal{Z}_{k,\ell}$ denotes the two compounded convolutions $\mathcal{Z}_k\mathcal{Z}_\ell$. More interestingly, the terms in the first line of the example residual (21) also forces a $\sigma\gamma$ correction to the evolution so that it becomes

$$\begin{aligned}\dot{\mathbf{U}}_j = & \frac{\gamma}{h^2}\delta^2\mathbf{U}_j - \frac{\gamma^2}{12h^2}\delta^4\mathbf{U}_j + \sigma\phi_{j,0} \\ & + \gamma\sigma\delta^2\left[-\frac{1}{24}\phi_{j,0} + \frac{1}{\pi^2}\sum_{k=2,\text{even}}^{\infty}\frac{1}{k^2}\phi_{j,k}\right] + \mathcal{O}(\sigma^3 + \gamma^3). \quad (24)\end{aligned}$$

The order of error comes from the terms present in the residuals but so far ignored when determining corrections. We ensure that the subgrid field \mathbf{u}_j is bounded, and the model evolution for the amplitudes \mathbf{U}_j does not have any incongruous fast time convolutions.

Continuing this iterative construction gives more asymptotically accurate models. The iteration terminates when the residuals are zero to some specified order. Then the Approximation Theorem of SCM theory [5, Theorem 8.1] assures us that the model has the same order of error as the residual.

3.4 Diffusion correlates noise across space

Because simple diffusion is linear, there are no stochastic interaction terms, those of $\mathcal{O}(\sigma^2)$, in the model (24). But note that the noise applied to the j th grid value \mathbf{U}_j is coupled to the noise sources in neighbouring elements through the second difference $\delta^2\phi_{j,k}$ terms in the second line of (24). This coupling arises because the noise in one element creates spatial structures that diffuse out into neighbouring elements and affect the evolution. The coupling in (24) does not depend upon element size because the diffusion time into a neighbouring element has the same time scale as diffusive decay within each element.

The analysis so far applies whether the forcing $\phi(\mathbf{x}, \mathbf{t})$ is deterministic or stochastic: the SDE (24) also models deterministic forcing. However, when the forcing components $\phi_{j,k}$ are independent stochastic processes then the model may be simplified as described in this and the next subsection.

The asymptotically approximate SDE (24) models forced diffusion dynamics, the SPDE (12), when we set the coupling parameter $\gamma = 1$. Undesirably, the resultant model has infinite sums of noise components:

$$\dot{\mathbf{U}}_j = \frac{1}{h^2}\delta^2\mathbf{U}_j - \frac{1}{12h^2}\delta^4\mathbf{U}_j + \sigma\phi_{j,0} + \sigma\delta^2\left[-\frac{1}{24}\phi_{j,0} + \frac{1}{\pi^2}\sum_{k=2,\text{even}}^{\infty}\frac{1}{k^2}\phi_{j,k}\right]. \quad (25)$$

But these noises are unknown. Thus we may combine the infinite sums of

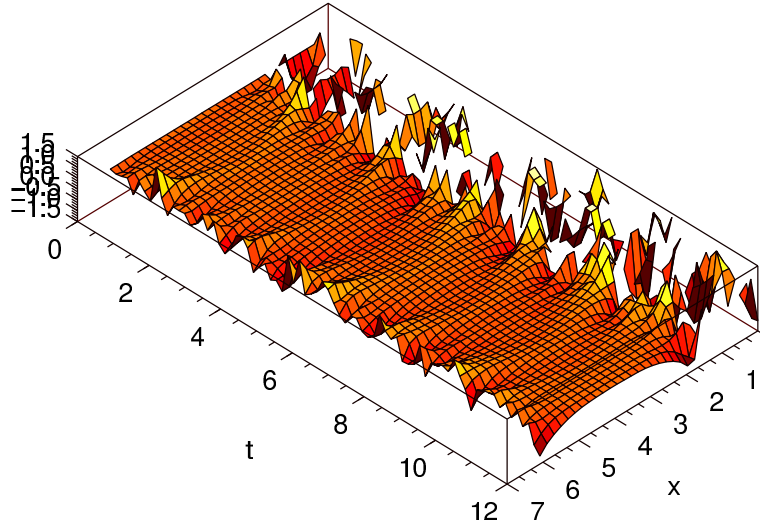


Figure 3: microscale simulation of the stochastically forced diffusion SPDE (12) ($\delta x = \pi/16$ and $\delta t = 0.01$ on a 2π -periodic domain). Restrict the large noise $10\phi(x, t)$, to one quarter of the domain, representing one macroscale element, and to the even modes, $\phi = \sum_{k=2, \text{even}}^{\infty} \phi_{1,k}(t) \cos k\theta$. The large noise in the element is mostly blanked out in the plot to highlight the relatively weak field diffusing out into the surrounding domain which correlates the *effective macroscale* noise as in (26).

noise terms into just two unknown noises with the same statistics as the infinite sums. I give two equivalent different versions.

1. The combination

$$\frac{1}{\pi^2} \sum_{k=2, \text{even}}^{\infty} \frac{1}{k^2} \phi_{j,k} \equiv \frac{1}{4\pi^2} \sqrt{\sum_{n=1}^{\infty} \frac{1}{n^4}} \hat{\phi}_j(t) = \frac{1}{12\sqrt{10}} \hat{\phi}_j(t)$$

where the effectively new stochastic noise $\hat{\phi}_j(t)$ represents the cumulative effect of the infinite sum of the stochastic components $\phi_{j,k}$ for k even. Thus the model SDE (25) becomes

$$\dot{U}_j = \frac{1}{h^2} \delta^2 U_j - \frac{1}{12h^2} \delta^4 U_j + \sigma \left[\phi_{j,0} - \frac{1}{24} \delta^2 \phi_{j,0} + \frac{1}{12\sqrt{10}} \delta^2 \hat{\phi}_j \right]. \quad (26)$$

Instead of the infinite number of noise processes in SDE (25), this model SDE has two independent noises for each element and hence only $2M$ noise modes for a spatial domain with M elements.

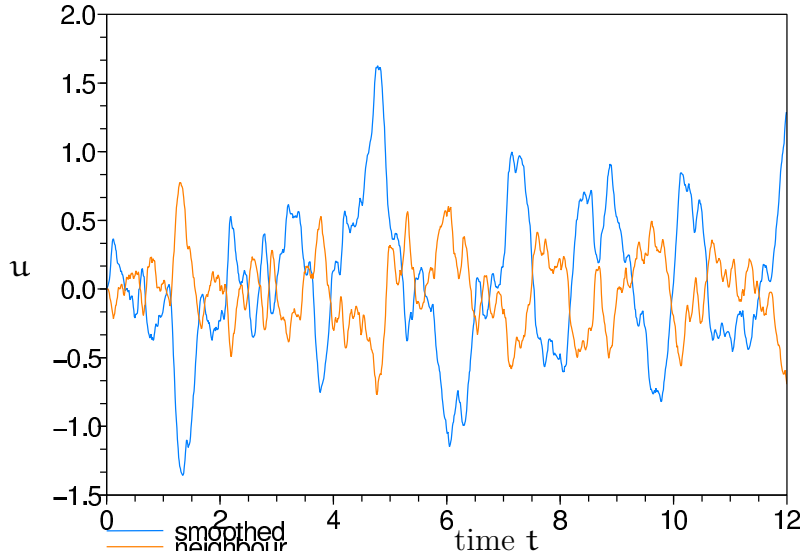


Figure 4: for the simulation shown in Figure 4, plot the smoothed “macroscale grid value” $u(\pi/4, t)$ and the neighbouring “macroscale grid value” $u(3\pi/4, t)$ as a function of time. The microscale stochastic forcing in one element generates the effectively opposite forcing in the neighbouring elements as predicted by (26).

The interesting and subtle component of the model (26) is $\frac{1}{12\sqrt{10}}\delta^2\hat{\phi}_j$. Numerical simulations confirm this component exists on the macroscopic scale. Usually its effects are masked by the dominant component $\phi_{j,0}$ and the non-contributing odd modes, so the numerical simulation plotted in Figure 3 is executed with $\phi_{j,k} = 0$ for $k = 0$ and for odd k . Also, Figure 3 applies the noise $\phi = \sum_{k=2, \text{even}}^{\infty} \phi_{1,k}(t) \cos k\theta$ to just one macroscale element, namely $0 < x < \pi/2$, to illuminate how the noise in any one element spreads its influence in space. See that although the large noise, $\sigma = 10$, induces fluctuations dominantly in the forced element, the noise also has a relatively weak effect external to the element. This external effect is modelled by the component $\delta^2\hat{\phi}_j$ in the SDE (26).

Simulations also confirm the amplitudes of the component $\sigma\frac{1}{12\sqrt{10}}\delta^2\hat{\phi}_j$. Figure 4 plots two grid values of the field $u(x, t)$ as a function of time t : one at the centre $x = \frac{1}{4}\pi$ of the forced element, $0 < x < \frac{1}{2}\pi$; and the other at the centre $x = \frac{3}{4}\pi$ of the adjacent element, $\frac{1}{2}\pi < x < \pi$. But recall that (26) models macroscopic space-time dynamics. Thus I smooth the microscopic time fluctuations of the grid value $u(\frac{1}{4}\pi, t)$ with

the normalised operator $\hat{\mathcal{Z}}_1 = [\mathcal{Z}_1 \mathbf{1}]^{-1} \mathcal{Z}_1$ that smooths over an inter-element diffusion time. Figure 4 shows that the smoothed grid value of the forced element has very much the same shaped fluctuations, but opposite and roughly twice the size of the fluctuations in the neighbouring grid value. This is as predicted by the model (26). Furthermore, the model predicts the standard deviation of the the two grid values should be $\sigma/6\sqrt{10} = .527$ and $\sigma/12\sqrt{10} = .264$. The simulation shown in Figure 4 has standard deviations .54 and .27, respectively, which are close enough considering the relatively few inter-element diffusion times simulated in the figure. *Such quantitative agreement between the subtleties of the SSM modelling and the numerical simulations strongly supports this approach to modelling SPDEs.*

2. A further slight simplification of the model combines the two second difference δ^2 terms through replacing the noise components by the orthogonal combination

$$\begin{bmatrix} \psi_j(t) \\ \hat{\psi}_j(t) \end{bmatrix} = \begin{bmatrix} \sqrt{\frac{5}{7}} & -\sqrt{\frac{2}{7}} \\ \sqrt{\frac{2}{7}} & \sqrt{\frac{5}{7}} \end{bmatrix} \begin{bmatrix} \phi_j(t) \\ \hat{\phi}_j(t) \end{bmatrix}.$$

Then the model (26) becomes

$$\dot{u}_j = \frac{1}{h^2} \delta^2 u_j - \frac{1}{12h^2} \delta^4 u_j + \sigma \left[\sqrt{\frac{5}{7}} \psi_j - \frac{1}{24} \sqrt{\frac{7}{5}} \delta^2 \psi_j + \sqrt{\frac{2}{7}} \hat{\psi}_j \right]. \quad (27)$$

Although both these models have $2M$ noise modes, Appendix A proves that we cannot reduce this to the minimal M modes without making the model undesirably nonlocal. SCM theory commends the particular weighted combination of noise in the model SDEs (26) or (27) as providing an appropriate balance between noise correlated between neighbouring elements and independent noise in each element as a discretisation for the stochastically forced diffusion equation (12).

3.5 Next nearest neighbour elements affect noise

Continue the analysis of the previous subsections to explore the example of stochastic diffusion (12) to terms in $\sigma\gamma^2$. These terms involve the forcing noise, coupling across five elements, and their interaction with diffusive dynamics. This section confirms the construction described in the previous section continues to higher order.

Computer algebra [50, §5] uses iteration to compute the SSM model. The iteration, based upon the processes explained in previous sections, terminates when the residuals of the forced diffusion equation (12) and the coupling ICCs (4) are zero to some specified order in the small parameters γ and σ . Then the Approximation Theorem for SPDEs [5, Theorem 8.1] assures us that the model is constructed to the same order of error. The main limitation of the computer algebra program [50] is that the infinite sums over Fourier modes must be truncated to finite sums. Extrapolating the patterns of coefficients from truncating to nine Fourier modes, the $\gamma^2\sigma$ correction to the SDE (25) forms the SDE model

$$\begin{aligned}\dot{u}_j = & \frac{\gamma}{h^2}\delta^2 u_j - \frac{\gamma^2}{12h^2}\delta^4 u_j + \sigma\phi_{j,0} + \gamma\sigma\delta^2 \left[-\frac{1}{24}\phi_{j,0} + \sum_{k=2,\text{even}}^{\infty} \frac{1}{\pi^2 k^2} \phi_{j,k} \right] \\ & + \gamma^2\sigma\delta^4 \left[\frac{17}{2880}\phi_{j,0} - \sum_{k=2,\text{even}}^{\infty} \left(\frac{1}{12\pi^2 k^2} + \frac{1}{\pi^4 k^4} \right) \phi_{j,k} \right] \\ & + \mathcal{O}(\sigma^3, \gamma^3).\end{aligned}\tag{28}$$

Again the infinite sums of unknown noise terms may be simplified. A little Gramm–Schmidt orthonormalisation² shows

$$\begin{bmatrix} \sum_{k=2,\text{even}}^{\infty} \frac{1}{\pi^2 k^2} \phi_{j,k} \\ \sum_{k=2,\text{even}}^{\infty} \left(\frac{1}{12\pi^2 k^2} + \frac{1}{\pi^4 k^4} \right) \phi_{j,k} \end{bmatrix} \equiv \begin{bmatrix} \frac{1}{12\sqrt{10}} & 0 \\ \frac{1}{112\sqrt{10}} & \frac{1}{5040\sqrt{2}} \end{bmatrix} \begin{bmatrix} \hat{\phi}_j(t) \\ \tilde{\phi}_j(t) \end{bmatrix},$$

for some new noises $\hat{\phi}_j(t)$ and $\tilde{\phi}_j(t)$ independent of $\phi_{j,0}$. Thus the model (28) is equivalent to

$$\begin{aligned}\dot{u}_j = & \frac{1}{h^2}\delta^2 u_j - \frac{1}{12h^2}\delta^4 u_j + \sigma \left[\phi_{j,0} - \frac{1}{24}\delta^2 \phi_{j,0} + \frac{17}{2880}\delta^4 \phi_{j,0} \right. \\ & \left. + \frac{1}{12\sqrt{10}}\delta^2 \hat{\phi}_j - \frac{1}{112\sqrt{10}}\delta^4 \hat{\phi}_j - \frac{1}{5040\sqrt{2}}\delta^4 \tilde{\phi}_j \right],\end{aligned}\tag{29}$$

upon also putting $\gamma = 1$ to recover a fully coupled model. It does not appear particularly useful to transform this model in order to reduce the number of differences δ appearing. The model SDE (29) extends the lower order model SDE (26) by including some fourth differences δ^4 . Such fourth differences of noise processes provides further subtle correlations among the noises in each element and how they affect the diffusive dynamics over long times.

²The Gramm–Schmidt orthonormalisation uses the sums $\sum_{n=1}^{\infty} n^{-4} = \pi^4/90$, $\sum_{n=1}^{\infty} n^{-6} = \pi^6/945$ and $\sum_{n=1}^{\infty} n^{-8} = \pi^8/9450$.

4 Nonlinear dynamics have irreducible noise interactions

Linear SPDEs with additive noise have SDE models which are also linear in the noise; for example, the forced diffusion SPDE (12) and its models such as (23), (28) and (29). Using the example of the forced Burgers' SPDE (1), we now explore general issues arising in the discretisation of the quite general nonlinear SPDE (6).

Consider the iterative construction of the stochastic slow manifold model to effects quadratic in the magnitude σ of the noise. We primarily seek two types of terms in the model: terms in σ^2 as these generate mean drift forcing from the noise; and also terms in $\sigma^2 \mathbf{U}_j$ as these reflect the influence of noise on the linear stability of Burgers' SPDE (1) [49, Figure 2] and [5, p.544].

4.1 Separate products of convolutions

In the iterative construction of a SSM we use the residuals of the governing SPDE to drive corrections, equation (13), to an approximate SSM model. In analysing a nonlinear SPDE (6), such as the stochastically forced Burgers' SPDE (1), products of memory convolutions appear in the residual. Furthermore, these convolutions will be over multiple time scales: even in the linear diffusion SPDE (12) the model (23) has double convolutions $\mathcal{Z}_{k,\ell}$. Just seeking terms quadratic in the noise magnitude σ we thus generally have to deal with quadratic products of multiple convolutions.

Obtain corrections from residuals To cater for the general case, define multiple convolutions. Let $\mathcal{Z}_{\mathbf{k}}$ denote the operator of multiple convolutions in time where vector \mathbf{k} indicates the decay rate of the corresponding convolution, that is, the operator

$$\mathcal{Z}_{\mathbf{k}} = \mathcal{Z}_{(k_1, k_2, \dots)} = \exp(-\beta_{k_1} \mathbf{t}) \star \exp(-\beta_{k_2} \mathbf{t}) \star \dots \star \quad \text{and} \quad \mathcal{Z} = 1, \quad (30)$$

in terms of the convolution (18); consequently

$$\partial_t \mathcal{Z}_{(k_1, k_2, \dots)} = -\beta_{k_1} \mathcal{Z}_{(k_1, k_2, \dots)} + \mathcal{Z}_{(k_2, \dots)}. \quad (31)$$

Note: the order of the convolutions does not matter [51, Appendix, e.g.]; however, keeping intact the order of the convolutions seems useful to most easily cancel like terms in the residual of the governing SPDE.

Recall that Sections 3.2–3.3 discuss how to determine updates \mathbf{u}'_j and \mathbf{g}'_j to the subgrid SSM field and the model SDE when the residual contains terms

linear in the noise: from (13) we may consider each term in the right-hand side in turn and solve equations of the form

$$\frac{\partial \mathbf{u}'_j}{\partial t} - \mathcal{L}\mathbf{u}'_j + \mathbf{g}'_j = \sigma \mathbf{f}_j(\mathbf{x}) \mathcal{Z}_{\mathbf{k}} \phi_{j,n}.$$

Sections 3.2–3.3 describe how to solve such equations. For nonlinear problems, such as the stochastically forced Burgers' SPDE (1), we additionally have to solve for corrections for each term of the form quadratic in the noise of the right-hand side of

$$\frac{\partial \mathbf{u}'_j}{\partial t} - \mathcal{L}\mathbf{u}'_j + \mathbf{g}'_j = \sigma^2 \mathbf{f}_j(\mathbf{x}) \mathcal{Z}_{\ell} \phi_{j,n} \mathcal{Z}_{\mathbf{k}} \phi_{i,m}.$$

As in Sections 3.2–3.3, two cases arise.

- Firstly, for each components of the subgrid structure $\mathbf{f}_j(\mathbf{x})$ in $\mathbf{v}_p(\mathbf{x})$ for wavenumber $p \geq 1$, there is no difficulty in simply including in the correction to the subgrid field the component

$$\sigma^2 \mathbf{v}_p(\mathbf{x}) \mathcal{Z}_p [\mathcal{Z}_{\ell} \phi_{j,n} \mathcal{Z}_{\mathbf{k}} \phi_{i,m}]$$

with its extra convolution in time.

- Secondly, for the component in $\mathbf{f}_j(\mathbf{x})$ that is constant across an element, the $\mathbf{v}_0(\mathbf{x})$ component, we separate the part of $\mathcal{Z}_{\ell} \phi_{j,n} \mathcal{Z}_{\mathbf{k}} \phi_{i,m}$ that has a bounded integral in time, and hence updates the subgrid field \mathbf{u}'_j , from the so-called secular part that does not have a bounded integral and hence must update the model SDE through \mathbf{g}'_j .

Integrate by parts to separate To extract quadratic corrections to the evolution, use integration by parts to reduce all non-integrable convolutions to the canonical form of the convolution being entirely over one of the noises in a quadratic term; that is, the canonical irreducible form is $\phi_{j,n} \mathcal{Z}_{\mathbf{k}} \phi_{i,m}$. To do this, rewrite the convolution ODE (31) as

$$\beta_{\mathbf{k}} \mathcal{Z}_{\mathbf{k}, \mathbf{k}'} = -\partial_t \mathcal{Z}_{\mathbf{k}, \mathbf{k}'} + \mathcal{Z}_{\mathbf{k}'},$$

where the vector of convolution parameters is $\mathbf{k} = \mathbf{k} \cdot \mathbf{k}'$ so that \mathbf{k} is the first component of vector \mathbf{k} , and \mathbf{k}' is the vector (if any) of the second and subsequent components of vector \mathbf{k} . Then for any ϕ and ψ

$$\int \mathcal{Z}_{\mathbf{k}, \mathbf{k}'} \phi \mathcal{Z}_{\ell} \psi \, dt$$

$$\begin{aligned}
&= \frac{1}{\beta_k + \beta_\ell} \int \beta_k \mathcal{Z}_{k,k'} \phi \mathcal{Z}_{\ell,\ell'} \psi + \mathcal{Z}_{k,k'} \phi \beta_\ell \mathcal{Z}_{\ell,\ell'} \psi \, dt \\
&= \frac{1}{\beta_k + \beta_\ell} \int [-\partial_t \mathcal{Z}_{k,k'} \phi + \mathcal{Z}_{k'} \phi] \mathcal{Z}_{\ell,\ell'} \psi + \mathcal{Z}_{k,k'} \phi [-\partial_t \mathcal{Z}_{\ell,\ell'} \psi + \mathcal{Z}_{\ell'} \psi] \, dt \\
&= \frac{1}{\beta_k + \beta_\ell} \int -\frac{\partial}{\partial t} [\mathcal{Z}_{k,k'} \phi \mathcal{Z}_{\ell,\ell'} \psi] + \mathcal{Z}_{k'} \phi \mathcal{Z}_{\ell,\ell'} \psi + \mathcal{Z}_{k,k'} \phi \mathcal{Z}_{\ell'} \psi \, dt \\
&= -\frac{1}{\beta_k + \beta_\ell} \mathcal{Z}_{k,k'} \phi \mathcal{Z}_{\ell,\ell'} \psi + \frac{1}{\beta_k + \beta_\ell} \int \mathcal{Z}_{k'} \phi \mathcal{Z}_{\ell,\ell'} \psi + \mathcal{Z}_{k,k'} \phi \mathcal{Z}_{\ell'} \psi \, dt.
\end{aligned}$$

Observe that each of the two components in the integrand on the last line above have one fewer convolutions than the initial integrand. Thus repeat this integration by parts until we reach terms of the form $\phi_{j,n} \mathcal{Z}_k \phi_{i,m}$ in the integrand. In this process, assign all the integrated terms to update the subgrid stochastic field \mathbf{u}'_j . The irreducible terms remaining in the integrand, those in the form $\phi_{j,n} \mathcal{Z}_k \phi_{i,m}$, must thus go to update the stochastic evolution \mathbf{g}'_j .

Computer algebra [50, §6] implements these steps in an iteration to derive the asymptotic series of the SSM of an SPDE.

4.2 Odd noise highlights nonlinear noise interactions

Section 3 shows that the subgrid modes with even wavenumber k were the only modes to affect the discretisation of the linear diffusion SPDE (12). The subgrid modes with odd wavenumber had no effect. This lack of effect is due to the left-right symmetry in the spatial diffusion. Thus, when coupling nonlinearity with diffusion, such as in Burgers' SPDE (1), restricting the forcing noise $\phi(\mathbf{x}, t)$ to have odd structure within each element highlights the *nonlinear* dynamics of the SPDE. This section reports on the successful modelling of Burgers' SPDE (1) for such odd noise. This section clarifies the modelling of subgrid nonlinear stochastic effects in the general SPDE (6).

Consider the simplest nontrivial case of Burgers' SPDE (1). This is the case of the noise $\phi(\mathbf{x}, t)$ having just the one Fourier component $\sin \theta$ in each element, *and* which is perfectly but oppositely correlated in neighbouring elements. But place no constraints on the time dependence although we only show simulations for independent 'white noise' in time. That is, in this section set the noise in each element to be

$$\phi(\mathbf{x}, t) = (-1)^j \phi_1(t) \sin \theta, \quad (32)$$

for the one 'white noise' $\phi_1(t)$. For example, Figure 5 shows a microscale simulation of Burgers' SPDE (1): as the macroscale element size $h = \pi/2$, the space-time structure of the noise reduces to simply $\phi_1(t) \cos 2\mathbf{x}$. We proceed

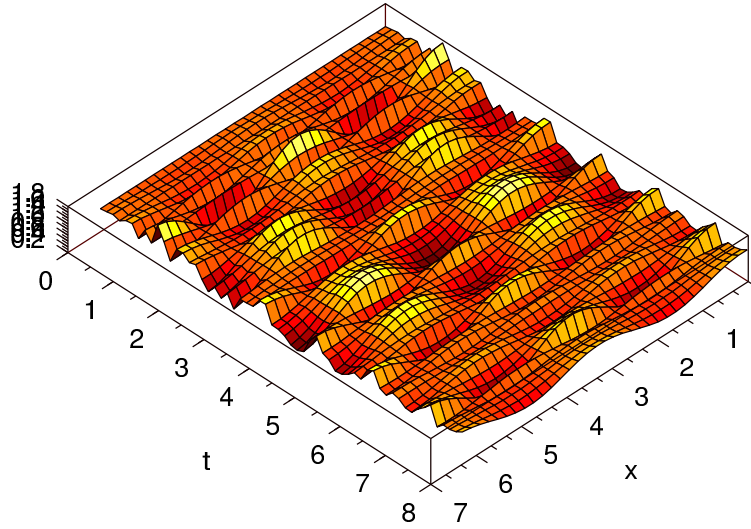


Figure 5: microscale simulation of one realisation of the stochastic field $u(x, t)$ when the applied noise is simply $\sigma\psi(t) \cos 2x$ for $\sigma = 1$ and nonlinearity $\alpha = \frac{1}{2}$. The macroscale grid points are at the nodes of this forcing, $x = \frac{1}{4}\pi, \frac{3}{4}\pi, \frac{5}{4}\pi, \frac{7}{4}\pi$, where the field u is relatively quiescent.

to model such microscale stochastic dynamics with elements of size $h = \pi/2$ centred at $X_j = (j - \frac{1}{2})\pi/2$. Figure 5 shows that the nodes of the stochastic forcing (32) are at these grid points X_j . Consequently, most methods for discretising Burgers' SPDE (1) on these elements would integrate over this noise and predict it has no influence. However, the nonlinear advection in Burgers' SPDE (1) carries the noise structure past the grid points and so generates fluctuations in the grid values: these fluctuations are hard to see in the simulation of Figure 5, but are clear in the plots of $u(X_2, t)$ in Figures 6 and 7. Holistic discretisation models the subgrid microscale dynamics and so predicts these fluctuations in the grid values.

Computer algebra constructs the SSM of Burgers' SPDE (1) with interelement coupling (4) [50]: just modify the code to the specific forcing (32). In each element the subgrid microscale field is

$$\begin{aligned} u = & u_j + \gamma \left[\frac{\theta}{\pi} \mu \delta + \frac{\theta^2}{2\pi^2} \delta^2 \right] u_j \pm \sigma \sin \theta \mathcal{Z}_1 \phi_1 \\ & \pm \sigma \alpha u_j \left[\frac{2h}{\pi^2} \mathcal{Z}_1 - \frac{4}{h} \left(\frac{1}{3} \cos 2\theta \mathcal{Z}_{2,1} - \frac{1}{15} \cos 4\theta \mathcal{Z}_{4,1} + \frac{1}{35} \cos 6\theta \mathcal{Z}_{6,1} \right) \right] \phi_1 \\ & + \mathcal{O}(\sigma^3 + \alpha^3 + \gamma^{3/2}), \end{aligned} \quad (33)$$

where even j is the upper alternative and odd j the lower. The first line of

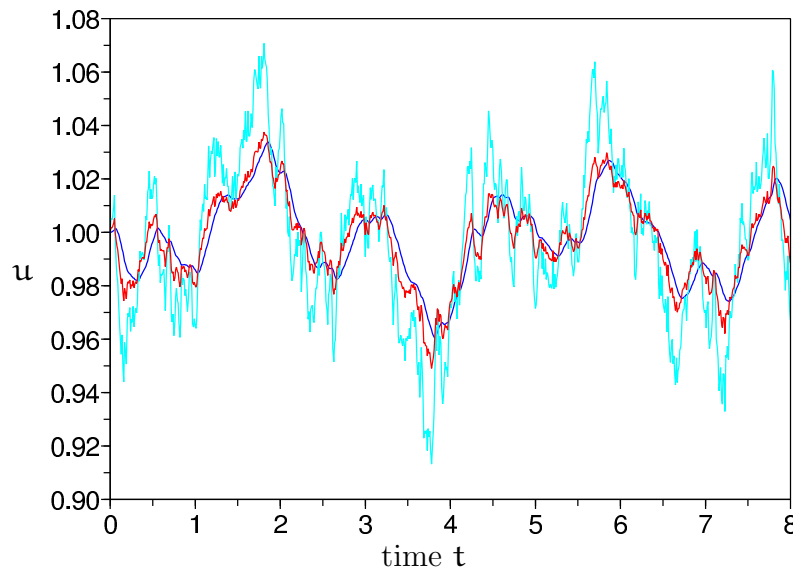


Figure 6: Compare the macroscale model (34) with a microscale simulation for small noise amplitude $\sigma = 0.3$ and nonlinearity $\alpha = \frac{1}{2}$: blue, the microscale field $u(x, t)$ at the macroscale grid point $x = X_2 = \frac{7}{4}\pi$ showing spatial structures carried by nonlinear advection past the grid point; cyan, the macroscale variable $U_2(t)$; and red, the macroscale SSM at the grid point, (35), for the shown $U_2(t)$ —the SSM and the microscale simulation match well.

the SSM (33) gives the deterministic Lagrangian interpolation among neighbouring grid values, when the coupling parameter $\gamma = 1$, and also gives the direct effects of the forcing noise in the memory convolution $\mathcal{Z}_1\phi_1$ with spatial structure $\sin\theta$. The second line of the SSM (33) begins to account for the nonlinear advection and interaction of these subgrid spatial structures: these processes transform the additive forcing into multiplicative noise, $U_j\phi_1$, with memory via the convolutions $\mathcal{Z}_{p,1}$.³ Higher order terms in the coupling γ , nonlinearity α and noise magnitude σ are too onerous to record for the microscale subgrid structures.

The evolution on the SSM (33) gives a holistic discretisation of Burgers' SPDE (1). To higher order in the small parameters, computer algebra gives

³Infinite sums in these nonlinear effects are truncated to the first eight Fourier components $1, \cos\theta, \dots, \cos 7\theta$. Higher wavenumber Fourier components could be resolved for this simple noise, but we do not for two reasons: crucial coefficients appear to be accurate to four decimal places with this truncation; and we cannot use higher wavenumbers when modelling the full spectrum of noise.

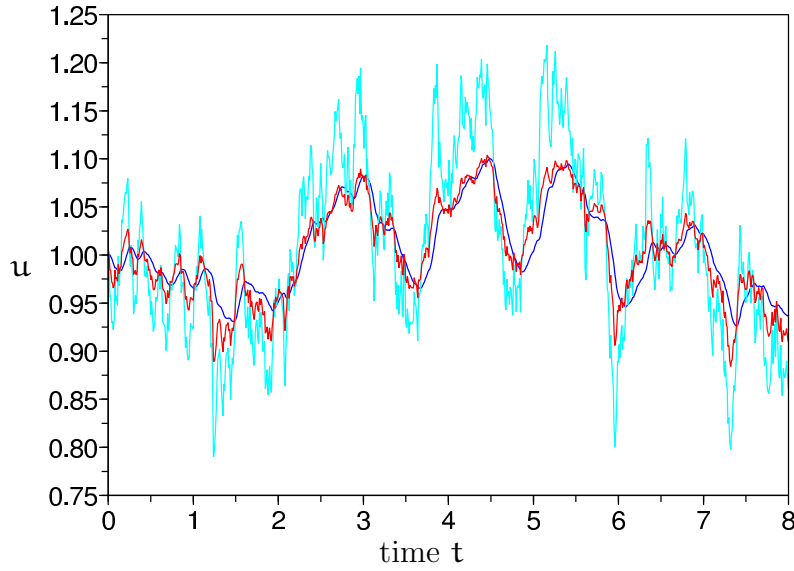


Figure 7: Compare the macroscale model (34) with a microscale simulation for larger noise amplitude $\sigma = 1$ and nonlinearity $\alpha = \frac{1}{2}$ (as for Figure 5): blue, the microscale field $u(x, t)$ at the macroscale grid point $x = X_2 = \frac{7}{4}\pi$ showing spatial structures carried by nonlinear advection past the grid point; cyan, the macroscale variable $U_2(t)$; and red, the macroscale SSM at the grid point, (35), for the shown $U_2(t)$ — the SSM and the microscale simulation match well.

that $U_j(t)$ evolve according to the SDEs

$$\begin{aligned}
 \dot{U}_j = & \frac{\gamma}{h^2} \delta^2 U_j - \frac{\gamma^2}{12h^2} \delta^4 U_j - \alpha \frac{\gamma}{h} U_j \mu \delta U_j + \alpha^2 \frac{\gamma}{12} U_j^2 \delta^2 U_j \\
 & \mp \sigma \alpha h \left[\frac{2}{\pi^2} U_j + \gamma (.1028 U_j + .0716 \delta^2 U_j) - .00363 \alpha^2 h^2 U_j^3 \right] \phi_1 \\
 & + \sigma^2 \alpha^2 \left[-\frac{8}{\pi^2} U_j \phi_1 \left(\frac{1}{15} Z_{2,1} + \frac{1}{255} Z_{4,1} + \frac{1}{1295} Z_{6,1} \right) \phi_1 \right. \\
 & \left. + 0.0195 h^2 U_j \phi_1 Z_1 \phi_1 \right] + \mathcal{O}(\sigma^5 + \alpha^5 + \gamma^{5/2}). \quad (34)
 \end{aligned}$$

The terms in the first line form the deterministic holistic discretisation of Burgers' equation discussed in [43]. Our interest lies in the noise terms on the second to fourth lines of the SDE (34). As for linear diffusion, we remove all memory convolutions from the terms linear in noise; these terms are recorded in the second line of the SDE (34). However, the terms quadratic in noise, σ^2 , must contain memory convolutions (as discussed in Section 4.1) in order to maintain (34) as a strong model of Burgers' SPDE (1).

Figures 6 and 7 show simulations of the discrete model SDE (34) for two different magnitudes σ of noise (cyan curves). Compare these to the blue curves of the field $u(X_2, t)$ at the corresponding grid point. Although the overall trends are roughly similar, the discretisation $U_2(t)$ is markedly different to $u(X_2, t)$. How can the SDE (34) be a strong model? Resolve the difference by recalling that to eliminate memory convolutions we must abandon the freedom to specify precisely the meaning of the amplitudes U_j ; see the discussion at the end of Section 3.2. Thus $U_2(t)$ and $u(X_2, t)$ need not agree. Instead field at a grid point, $u(X_j, t)$, must be predicted by the SSM (33) evaluated at the grid points, namely

$$\begin{aligned} u(X_j, t) = & U_j \pm \sigma \alpha U_j \left[\frac{2h}{\pi^2} \mathcal{Z}_1 - \frac{4}{h} \left(\frac{1}{3} \mathcal{Z}_{2,1} - \frac{1}{15} \mathcal{Z}_{4,1} + \frac{1}{35} \mathcal{Z}_{6,1} \right) \right] \phi_1 \\ & + \mathcal{O}(\sigma^4 + \alpha^4 + \gamma^2). \end{aligned} \quad (35)$$

Figures 6 and 7 plot the SSM predicted grid value (35) in red and display a good agreement with the microscale simulation (blue).⁴

Evidently, SCM theory successfully supports discrete models of SPDEs.

4.3 Strong models of stochastic dynamics are complex

Now look at the details of the discrete model of the stochastically forced Burgers' SPDE (1). Computer algebra [50] derives the following leading terms in the asymptotic series of the model $\dot{U}_j = g_j(\mathbf{U}, t, \epsilon)$. The large amount of algebraic detail reflects the large complexity of the multiple physical processes acting on the subgrid microscale structures forced by the rich stochastic spectrum of noise. Fortunately the arguments of the next section simplify the model significantly. Scan past the following model to the discussion following.

$$\begin{aligned} \dot{U}_j = & \gamma \frac{1}{h^2} \delta^2 U_j - \gamma^2 \frac{1}{12h^2} \delta^4 U_j - \gamma \alpha \frac{1}{h} U_j \mu \delta U_j \\ & + \sigma \left\{ \left[1 - \gamma \frac{1}{24} \delta^2 + \gamma^2 \left(\frac{3}{640} + \frac{1}{8\pi^4} \right) \delta^4 \right] \phi_{j,0} \right. \\ & + \left[\gamma \frac{1}{4\pi^2} \delta^2 - \gamma^2 \left(\frac{1}{48\pi^2} + \frac{1}{16\pi^4} \right) \delta^4 \right] \phi_{j,2} - \alpha \frac{2h}{\pi^2} U_j \phi_{j,1} \\ & + \alpha \gamma \frac{1}{h^2 \pi^2} \left[U_j \left(\frac{8}{\pi^2} \mu \delta \phi_{j,0} - \frac{1}{4} \mu \delta \phi_{j,2} + \left(\frac{1}{12} + \frac{5}{3\pi^2} \right) \delta^2 \phi_{j,1} \right) \right. \\ & \left. \left. + \mu \delta U_j \left(\frac{1}{4} \phi_{j,2} + \left(\frac{1}{6} + \frac{10}{3\pi^2} \right) \mu \delta \phi_{j,1} \right) \right] \right\} \end{aligned}$$

⁴In stochastic systems there appears to be a remarkably big difference between the discretisation variables $U_j(t)$ and the microscale grid values $u(X_j, t)$.

$$\begin{aligned}
& -\delta^2 \mathcal{U}_j \left(\left(\frac{1}{6} + \frac{1}{3\pi^2} \right) \phi_{j,1} - \left(\frac{1}{24} + \frac{5}{6\pi^2} \right) \delta^2 \phi_{j,1} \right) \Big] \\
& - \alpha^2 \frac{8h^2}{3\pi^4} \mathcal{U}_j^2 \phi_{j,0} \Big\} \\
& + \sigma^2 \left\{ \alpha \frac{h}{\pi^2} \left[-2\phi_{j,0} \mathcal{Z}_1 \phi_{j,1} + \frac{2}{5} \phi_{j,1} \mathcal{Z}_2 \phi_{j,2} + \frac{2}{5} \phi_{j,2} \mathcal{Z}_1 \phi_{j,1} \right] \right. \\
& + \alpha \gamma \frac{1}{h\pi^2} \left(-32\phi_{j,0} \mathcal{Z}_{1,2} \mu \delta - \frac{4}{5} \phi_{j,1} \mathcal{Z}_{2,2} \delta^2 + \frac{32}{5} \phi_{j,2} \mathcal{Z}_{1,2} \mu \delta \right) \phi_{j,2} \\
& + \alpha \gamma \frac{h}{\pi^2} \left[\phi_{j,0} \left(\frac{8}{\pi^2} \mathcal{Z}_1 \mu \delta (\phi_{j,0} + \phi_{j,2}) + \left(\frac{1}{12} + \frac{5}{3\pi^2} \right) \mathcal{Z}_1 \delta^2 \phi_{j,1} \right. \right. \\
& \quad \left. \left. - \left(\frac{1}{4} + \frac{8}{\pi^2} \right) \mathcal{Z}_2 \mu \delta \phi_{j,2} \right) + \phi_{j,1} \mathcal{Z}_2 \left(\frac{1}{5} \delta^2 \phi_{j,0} - \left(\frac{1}{20} + \frac{13}{150\pi^2} \right) \phi_{j,2} \right) \right. \\
& \quad \left. + \phi_{j,2} \left(-\frac{8}{5\pi^2} \mathcal{Z}_1 \mu \delta (\phi_{j,0} + \phi_{j,2}) - \left(\frac{1}{60} + \frac{17}{75\pi^2} \right) \mathcal{Z}_1 \delta^2 \phi_{j,1} \right. \right. \\
& \quad \left. \left. + \left(\frac{1}{8} + \frac{4}{5\pi^2} \right) \mathcal{Z}_2 \mu \delta \phi_{j,2} \right) \right. \\
& \quad + \delta^2 \phi_{j,0} \mathcal{Z}_1 \left(-\left(\frac{1}{12} + \frac{2}{15\pi^2} \right) + \left(\frac{1}{24} + \frac{5}{6\pi^2} \right) \delta^2 \right) \phi_{j,1} \\
& \quad - \delta^2 \phi_{j,1} \mathcal{Z}_2 \left(\left(\frac{1}{60} + \frac{17}{75\pi^2} \right) + \left(\frac{1}{120} + \frac{17}{150\pi^2} \right) \delta^2 \right) \phi_{j,2} \\
& \quad - \delta^2 \phi_{j,2} \mathcal{Z}_1 \left(\left(\frac{1}{20} + \frac{44}{75\pi^2} \right) + \left(\frac{1}{120} + \frac{17}{150\pi^2} \right) \delta^2 \right) \phi_{j,1} \\
& \quad + \mu \delta \phi_{j,0} \left(\left(\frac{1}{6} + \frac{10}{3\pi^2} \right) \mathcal{Z}_1 \mu \delta \phi_{j,1} + \left(\frac{1}{4} - \frac{8}{5\pi^2} \right) \mathcal{Z}_2 \phi_{j,2} \right) \\
& \quad - \mu \delta \phi_{j,1} \left(\frac{1}{30} + \frac{34}{75\pi^2} \right) \mathcal{Z}_2 \mu \delta \phi_{j,2} \\
& \quad + \mu \delta \phi_{j,2} \left(-\left(\frac{1}{30} + \frac{34}{75\pi^2} \right) \mathcal{Z}_1 \mu \delta \phi_{j,1} + \left(\frac{1}{8} - \frac{4}{5\pi^2} \right) \mathcal{Z}_2 \phi_{j,2} \right) \Big] \\
& + \alpha^2 \frac{1}{\pi^2} \mathcal{U}_j \left[-\frac{16}{3} \phi_{j,0} \left(2\mathcal{Z}_{1,2} + \frac{h^2}{\pi^2} \mathcal{Z}_2 \right) \phi_{j,2} \right. \\
& \quad \left. - \frac{8}{15} \phi_{j,1} \left(\mathcal{Z}_{2,1} - \frac{4h^2}{\pi^2} \mathcal{Z}_1 \right) \phi_{j,1} + \frac{16}{15} \phi_{j,2} \left(2\mathcal{Z}_{1,2} + \frac{h^2}{\pi^2} \mathcal{Z}_2 \right) \phi_{j,2} \right] \Big\} \\
& + \mathcal{O}(\sigma^3, \alpha^3 + \gamma^3). \tag{36}
\end{aligned}$$

The model resolves noise, nonlinearity and inter-element interactions The model SDE (36) is computed to residuals $\mathcal{O}(\sigma^3, \alpha^3 + \gamma^3)$ and hence the model has this order of error. The truncation to errors $\mathcal{O}(\sigma^3)$ ensures the model retains the interesting quadratic noise interaction terms parametrised by σ^2 seen in the last 14 lines of the SDE (36). The truncation to error $\mathcal{O}(\alpha^3 + \gamma^3)$ resolves linear dynamics within and between next nearest neighbour elements, and nonlinear dynamics within and between nearest neighbour elements.

Truncate to three Fourier modes The model SDE (36), complicated as it is, resolves just the first three Fourier modes of the forcing noise, namely $\phi = \sum_{k=0}^2 \phi_{j,k}(\mathbf{t}) \text{csn } k\theta$. Similarly, the model (36) only resolves subgrid microscale structure in the same three Fourier modes. In principle, the com-

Table 1: number of terms in the evolution $\dot{\mathbf{U}}_j = \mathbf{g}_j(\mathbf{U}, \mathbf{t}, \boldsymbol{\epsilon})$ when only three Fourier modes are used for the subgrid stochastic structures: the numbers in *italics* count the terms in the model SDE (36). Expect many more terms when using more Fourier modes. Blank entries in the table are unknown.

σ^0					σ^1					σ^2				
α^3	0	0			α^3	1	13			α^3	9			
α^2	0	3	14		α^2	1	16	82		α^2	6	156		
α^1	0	2	8	19	α^1	1	11	45	93	α^1	3	42	238	
α^0	0	3	5	7	α^0	1	6	10	14	α^0	0	0	0	0
	γ^0	γ^1	γ^2	γ^3		γ^0	γ^1	γ^2	γ^3		γ^0	γ^1	γ^2	γ^3

puter algebra [50] could generate models with many more subgrid microscale modes; however, computer memory currently limits me to three modes for this analysis of the forced Burgers' SPDE (1).

Table 1 indicates the level of complexity of the multiparameter asymptotic series via a type of Newton diagram. The table reports the number of terms in various parts of the model $\dot{\mathbf{U}}_j = \mathbf{g}_j(\mathbf{U}, \mathbf{t}, \boldsymbol{\epsilon})$, there are vastly more terms describing the subgrid microscale structure $\mathbf{u}_j(\mathbf{U}, \mathbf{x}, \mathbf{t}, \boldsymbol{\epsilon})$ within each element. The critical point is that *if we pursue either higher order truncations, or more Fourier modes, then the complexity of the model increases alarmingly*. Thus, for the moment, I choose to truncate the model as in (36).

Linear diffusion is a subset The diffusion model SDE (28) appears in the first three lines of the nonlinear model (36) when the nonlinearity parameter $\alpha = 0$. The only differences are due to the finite truncation of the Fourier modes in this section: the infinite sums do not appear; and the coefficient of the $\gamma^2 \sigma \delta^4 \phi_{j,0}$ term has a small error from the modal truncation. The nonlinear modelling builds on the model SDE of linear diffusion.

Abandon fast time convolutions The undesirable feature of the large time model (36) is the inescapable appearance in the quadratic noise terms of fast time convolutions, such as $\mathcal{Z}_1 \phi_{j,1} = \exp(-\beta_1 \mathbf{t}) \star \phi_1$ and $\mathcal{Z}_{1,2} \phi_{j,2} = \exp(-\beta_1 \mathbf{t}) \star \exp(-\beta_2 \mathbf{t}) \star \phi_{j,2}$. These require resolution of the subgrid fast time scales in order to maintain fidelity with the original Burgers' SPDE (1) and so require incongruously small time steps for a supposedly slowly evolving model. However, maintaining fidelity with the details of the white noise source $\phi(\mathbf{x}, \mathbf{t})$ is a pyrrhic victory when we are only interested in the relatively slow long term dynamics. Instead we need only those parts of the quadratic noise factors, such as $\phi_{j,0} \mathcal{Z}_1 \phi_{j,1}$ and $\phi_{j,0} \mathcal{Z}_{1,2} \phi_{j,2}$, that *over the long*

macroscopic time scales are firstly correlated with the other processes that appear and secondly independent of the other processes. The next section explores how these components of the quadratic noises not only introduce factors of effectively *new independent* noises into the model, but also introduce a deterministic drift due to stochastic resonance (as also noted by Drolet & Vinal [17]).

5 Stochastic resonance influences deterministic dynamics

Chao & Roberts [11, 49, 51] argued that quadratic terms involving memory integrals of the noise were effectively new drift and new noise terms when viewed over the long time scales of the relatively slow evolution of a model such as the SDE (36). The arguments rely upon the noise being stochastic white noise. The strong model SDE (36) faithfully tracks any given realisation of the original Burgers' SPDE (1) [5, Theorem 7.1(i), e.g.] whether the forcing is deterministic or stochastic; however, now we derive a weak model for the case of stochastic forcing. The weak model only maintains fidelity to solutions of the original Burgers' SPDE (1) in a weak sense—we cannot know which realisations ensure a match between the model and Burgers' SPDE because of the effectively new noises on the macroscale of the model.

Analogously, Just et al. [27] argued that fast time deterministic chaos appears as noise when viewed over long time scales. In the case of deterministic forcing of Burgers' equation (1), perhaps similar arguments to those of Just et al. could also map the strong model SDE (36), with its troublesome fast time convolutions, into a stochastic model over the large time scales of interest.

5.1 Canonical quadratic noise interactions

In the strong model (36) we need to understand and summarise the long term effects of the quadratic noises that appear in the form $\phi_j \mathcal{Z}_k \phi_i$ and $\phi_j \mathcal{Z}_{k,\ell} \phi_i$, where in this section ϕ_i and ϕ_j represent the various possibilities for the components $\phi_{j,k}$. The noises ϕ_i and ϕ_j may be independent or they may be the same process depending upon the term under consideration. We aim to replace such noise terms by a corresponding stochastic differential $d\mathbf{y}/dt$ for a Stratonovich stochastic process \mathbf{y} with some drift and volatility: $d\mathbf{y} = (\cdot)dt + (\cdot)dW$ for a Wiener process W . Thus we must understand the long term dynamics of Stratonovich stochastic processes \mathbf{y}_1 and \mathbf{y}_2 defined via the

SDEs

$$\frac{dy_1}{dt} = \phi_j \mathcal{Z}_k \phi_i \quad \text{and} \quad \frac{dy_2}{dt} = \phi_j \mathcal{Z}_{\ell,k} \phi_i. \quad (37)$$

Use the argument in [51] to proceed. Name the two convolutions that appear in the nonlinear terms (37) as $z_1 = \mathcal{Z}_k \phi_i$ and $z_2 = \mathcal{Z}_{\ell,k} \phi_i$. They satisfy the SDEs (22). Now put the SDEs (37) and (22) together: we must understand the long term properties of y_1 and y_2 governed by the coupled system

$$\begin{aligned} \dot{y}_1 &= z_1 \phi_j, & \dot{z}_1 &= -\beta_k z_1 + \phi_i, \\ \dot{y}_2 &= z_2 \phi_j, & \dot{z}_2 &= -\beta_\ell z_2 + z_1. \end{aligned} \quad (38)$$

There are two cases labelled by s to consider: when $i = j$ the two source noises ϕ_i and ϕ_j are identical, $s = 1$; whereas when $i \neq j$ the two noise sources are independent, $s = 0$.

Deterministic centre manifold theory applied to the Fokker–Planck equation for the system (38) proves [51, §4] that as time $t \rightarrow \infty$ the probability density function (PDF) for the SDE (38) tends to a quasi-stationary distribution [39]:

$$\begin{aligned} P(\mathbf{y}, \mathbf{z}, t) &\rightarrow A \exp \left\{ -(\beta_k + \beta_\ell) [z_1^2 - 2\beta_\ell z_1 z_2 + \beta_\ell (\beta_k + \beta_\ell) z_2^2] \right\} \\ &\times \left\{ p - s [z_1^2 - 2\beta_\ell z_1 z_2 + 2\beta_\ell (\beta_k + \beta_\ell) z_2^2 + B_1] \frac{\partial p}{\partial y_1} \right. \\ &\quad \left. - s [(\beta_k + \beta_\ell) z_2^2 + B_2] \frac{\partial p}{\partial y_2} + \dots \right\}, \end{aligned} \quad (39)$$

exponentially quickly for some normalisation constants A , B_1 and B_2 , and for some evolving $p(\mathbf{y}, t)$.

Interpret $p(\mathbf{y}, t)$ as a type of conditional probability density. Simultaneously with finding the next order corrections to this PDF $P(\mathbf{y}, \mathbf{z}, t)$, I found in [51] that the relatively slowly varying, quasi-conditional probability density p evolves according to the Kramers–Moyal expansion [37, 36, 56, e.g.]

$$\frac{\partial p}{\partial t} = -\frac{1}{2}s \frac{\partial p}{\partial y_1} + \frac{1}{4\beta_k} \begin{bmatrix} 1 & \frac{1}{\beta_k + \beta_\ell} \\ \frac{1}{\beta_k + \beta_\ell} & \frac{1}{\beta_\ell (\beta_k + \beta_\ell)} \end{bmatrix} : \nabla \nabla p + \dots \quad (40)$$

The deterministic centre manifold relevance theorem [48, §2.2.2, e.g.] assures us that this PDE for the evolution of the quasi-PDF $p(\mathbf{y}, t)$ models the dynamics of the PDF of (38) for large time. The PDE (40) is thus a weak model of the evolution of noises interacting nonlinearly with each other.

5.2 Translate to a corresponding SDE

Interpret the shown terms of the Kramers–Moyal PDE (40) as a Fokker–Planck equation for the SDEs

$$\dot{\mathbf{y}}_1 = \frac{1}{2}\mathbf{s} + \frac{\psi_1(\mathbf{t})}{\sqrt{2\beta_k}} \quad \text{and} \quad \dot{\mathbf{y}}_2 = \frac{1}{\beta_k + \beta_\ell} \left(\frac{\psi_1(\mathbf{t})}{\sqrt{2\beta_k}} + \frac{\psi_2(\mathbf{t})}{\sqrt{2\beta_\ell}} \right). \quad (41)$$

Of course there are many coupled SDEs like these whose Fokker–Planck equation is the PDE (40): for example, Just et al. [27] choose the matrix of volatilities to be the positive definite, symmetric square root of the diffusivity matrix in the PDE (40). For our purposes any of the possible volatility matrices would suffice: in constructing a weak model via the Fokker–Planck equations we necessarily lose fidelity of paths, and now only require fidelity of distributions and correlations. The Cholesky decomposition of the symmetric diffusivity matrix reduces the number of stochastic terms in the SDEs (41), and hence reduces the number of stochastic terms in the eventual weak model SDE. Furthermore, the Cholesky decomposition also ensures that if we were to analyse the dynamics of Burgers’ SPDE (1) to higher orders, then the higher order convolutions of noise that would arise do not change the 2×2 Cholesky decomposition leading to (41) [51, §5]. Thus the SDEs (41) are our model for the evolution of the irreducible noise convolutions (37) over long times.

As argued by Chao & Roberts [11, 49] and proved in [51, Appendix], the two $\psi_i(\mathbf{t})$ are new noises independent of ϕ_i and ϕ_j *over long time scales*. The remarkable feature to see in the SDEs (41) is that for the case of identical noise, $\phi_i = \phi_j$ ($s = 1$), there is a mean drift $\frac{1}{2}$ in the stochastic process \mathbf{y}_1 ; there is no mean drift in any other process nor in the other case of independent ϕ_i and ϕ_j , ($s = 0$).

You might wonder about the role of the neglected terms, indicated by the ellipsis \dots , in the Kramers–Moyal expansions of the PDF (39) and the proposed Fokker–Planck PDE (40). In the PDF (39) the neglected terms just provide more details of the non-Gaussian structure of the PDF in the slowly evolving long time dynamics. The effects of the neglected terms in the PDE (40) correspond to algebraically decaying departures from the second order truncation. Such algebraically decaying transients may represent slow decay of non-Markovian effects among the \mathbf{y} variables. However, the truncation (40) that we interpret as a Fokker–Planck PDE is the lowest order *structurally stable* model and so will adequately model the dynamics of \mathbf{y}_1 and \mathbf{y}_2 over the longest time scales. Just et al. [27], in their equation (11), similarly truncate to second order.

5.3 Transform the detailed strong model to be usefully weak.

The quadratic noises in the strong model SDE (36) involve the convolutions \mathcal{Z}_1 and \mathcal{Z}_2 which have respective decay rates $\beta_1 = \pi^2/h^2$ and $\beta_2 = 4\pi^2/h^2$. Thus, via various instances of the SDEs (41), to obtain a model for *long time scales* we replace the quadratic noises in (36) as follows:

$$\begin{aligned}\phi_{j,n}\mathcal{Z}_k\phi_{i,m} &\mapsto \frac{1}{2}\delta_{ij}\delta_{mn} + \frac{h}{k\pi\sqrt{2}}\psi_{nmk}(t), \\ \phi_{j,n}\mathcal{Z}_{k,\ell}\phi_{i,m} &\mapsto \frac{h^3}{\pi^3(k^2 + \ell^2)} \left[\frac{1}{\ell\sqrt{2}}\psi_{nm\ell}(t) + \frac{1}{k\sqrt{2}}\psi_{nmk}(t) \right],\end{aligned}\quad (42)$$

where ψ_{nmk} and $\psi_{nm\ell}$ are the effectively new and *independent* white noises, that is, derivatives of new independent Wiener processes. In the above I omit the subscripts of i and j on ψ and henceforth on ϕ because they are redundant when we record the model using centred mean and difference operators. Note that δ_{ij} and δ_{mn} , with its pair of subscripts, do *not* denote a centred difference but rather denote the Dirac delta to cater for the case of the self interaction of a noise when there is a mean drift effect.

Computer algebra [50, §9] implements the transformations (42) to the strong model SDE (36) to derive the corresponding weak model SDE

$$\begin{aligned}\dot{U}_j = & \gamma \frac{1}{h^2} \delta^2 U_j - \gamma^2 \frac{1}{12h^2} \delta^4 U_j - \gamma \alpha \frac{1}{h} U_j \mu \delta U_j \\ & + \sigma [\phi_0 - .0206\alpha h U_j \phi_1 - .02738\alpha^2 h^2 U_j^2 \phi_2] \\ & + \gamma \sigma \delta^2 (-.04167\phi_0 + .02533\phi_2) + \gamma^2 \sigma \delta^4 (.005971\phi_0 - .002752\phi_2) \\ & + \alpha h \gamma \sigma \{ \mu \delta U_j [.02533\phi_2 + .05111\mu \delta \phi_1] \\ & + \delta^2 U_j [-.02031\phi_1 + .01278\delta^2 \phi_1] \\ & + U_j [\mu \delta (.08213\phi_0 - .02533\phi_2) + .02555\delta^2 \phi_1] \} \\ & + \alpha h^2 \sigma^2 (-.04561\psi_{011} + .004561\psi_{122} + .009122\psi_{211}) \\ & + \alpha h^2 \gamma \sigma^2 [\mu \delta_2 (.01849\psi_{001} + .01849\psi_{021} - .01479\psi_{0212} - .01949\psi_{022} \\ & - .003697\psi_{201} - .003697\psi_{221} + .002958\psi_{2212} + .003828\psi_{222}) \\ & + \mu \delta_1 (.001002\psi_{022} + .0005011\psi_{222}) \\ & + \mu \delta_1 \mu \delta_2 (.0115\psi_{011} - .0009038\psi_{122} - .001808\psi_{211}) \\ & + \delta_2^2 (.005752\psi_{011} + .0002311\psi_{102} - .0007858\psi_{122} \\ & - .0001155\psi_{1222} - .0009038\psi_{211}) \\ & + \delta_1^2 (-.002209\psi_{011} - .0004519\psi_{122} - .002496\psi_{211}) \\ & + \delta_1^2 \delta_2^2 (.002876\psi_{011} - .000226\psi_{122} - .0004519\psi_{211})]\end{aligned}$$

$$\begin{aligned}
& + \alpha^2 h^3 \sigma^2 \mathbf{U}_j (-.004929\psi_{0212} - .008626\psi_{022} + .004929\psi_{111} \\
& \quad - .0002465\psi_{1112} - .0001232\psi_{112} + .0009859\psi_{2212} + .001725\psi_{222}) \\
& + .01643\alpha^2 h^2 \sigma^2 \mathbf{U}_j + \mathcal{O}(\sigma^3, \alpha^3 + \gamma^3), \tag{43}
\end{aligned}$$

where $\mu\delta_1$ and δ_1^2 denote differences in the first grid variable implicit in the noises ψ , whereas $\mu\delta_2$ and δ_2^2 denote differences in the second implicit grid variable. The value of the weak model SDE (43) is that it has no fast time scale processes: it is truly a model of the long time dynamics. Of course the fluctuating processes ϕ_n and ψ_{nmk} have fluctuations over all time scales, but we know how to integrate these with macroscopic time steps [29, e.g.]. The complexity of the weak model SDE (43) reflects the many intricacies of the inter-element interactions and the subgrid microscale processes resolved in this rigorous approach to forming discretisations of SPDEs.

The stochastic components of the weak model SDE (43), and the strong model SDE (36), are actually more complex than it might appear: the difference operators hide a lot of detail. Any one apparent noise source ψ_{nmk} actually represents $5M$ independent noise sources over all the M elements. In order to clarify all the discrete differences of ψ_{nmk} that appear, temporarily reinstate the implicit subscripts. For the j th element we need the nine noise components ψ_{jjnmk} , $\psi_{j\pm 1,jnmk}$, $\psi_{j,j\pm 1,nmk}$ and $\psi_{j\pm 1,j\pm 1,nmk}$ in order to compute all the differences that appear in the SDE (43). Of these, seven of the noises are used in computing the differences in the $(j \pm 1)$ th element, and two are also used in computing the differences in the $(j \pm 2)$ th element. Consequently each of the $\sigma^2\gamma$ noises that appear in the SDE (43) actually represent, in nett effect, five independent noise sources for each element. Such terms reflect subtle cross-correlations between the stochastic dynamics within neighbouring finite elements.

Stochastic induced drift affects stability The terms quadratic in the noise magnitude, indicated by a factor σ^2 , are particularly complicated. With relatively small numerical coefficient perhaps we could ignore them—except one important term. The last known term in the SDE (43), namely $+.01643\alpha^2 h^2 \sigma^2 \mathbf{U}_j$, is a *mean* effect of the noise interacting through the non-linearity. The positive coefficient of this term shows that the self interactions of each of the many subgrid microscale noises actually act to promote growth of macroscale structures in the dynamics of Burgers' SPDE (1). For many practical purposes we could probably ignore all the σ^2 terms except this one term because of its potential macroscopic effects over long times. Indeed, because of its potential importance, I included this mean effect in the introductory model SDE (5).

Similarly, Boxler [5, p.544], Drolet & Vinals [17, 18] and Knobloch & Weisenfeld [30] and Vanden-Eijnden [57, p.68] found stability modifying linear terms in their analyses of stochastically perturbed bifurcations and other nonlinear systems. Recall that the Relevance Theorem by Boxler [5, Theorem 7.3(a)] proves that the stability of an original SDE is the same as the model SDE on the SCM; thus growth promoting terms in a model SDEs do represent dynamics of an SPDE (6). Analogously to these effects of microscale noise on the macroscale dynamics, Just et al. [27] sought to determine how microtime deterministic chaos, not noise, translates into a new effective stochastic noise in the slow modes of a deterministic dynamical system. The analysis here shows that noise in many subgrid modes contribute to reduce the stability of the trivial equilibrium $\mathbf{u} = \mathbf{0}$ in Burgers' SPDE (1).

5.4 Consolidate the new noise

Orthonormalisation simplifies the representation of the effects of all the noise terms in the weak model SDE (43): this section reduces the 16 quadratic noises to just seven equivalent noise sources. Because the noise terms appearing in (43) are unknown in detail, we may replace linear combinations of them by one equivalent noise term as Sections 3.4 and 3.5 did for the model of linear diffusion. Recall that we have to be careful to maintain the correct correlations between the various places that the noise terms appear. The situation is fiendishly more complicated in the highly complex model (43) for the nonlinear Burgers' SPDE (1), in comparison to the earlier diffusion SPDE (12), because the noises appear in many more places in different combinations (indicated by the parenthetical groupings in (43)).

- Because of the severe truncation in the number of retained Fourier modes, there is no significant simplification possible in the terms linear in the noise magnitude σ : the ϕ_n noises just occur in too many places; if we had resolved the infinite sum of Fourier modes, as in Section 3.4 and 3.5, then the infinite noise components perhaps would be reduced to the form of the weak model SDE (43).
- Now turn to the quadratic noise terms in the SDE (43). Computer algebra [50, §9] extracts the eight different combinations of noises ψ in the SDE (43). Then a Gramm–Schmidt orthonormalisation of the vectors of coefficients is essentially a QR decomposition of the transpose of the matrix of noise coefficients: namely, factor the noise contributions to $\mathbf{R}^T \mathbf{Q}^T \psi$ where ψ is the vector of noise processes, \mathbf{Q}^T is an orthogonal matrix, and \mathbf{R}^T is a lower triangular matrix. Then $\chi = \mathbf{Q}^T \psi$ are a vector

of new independent noise processes to replace $\boldsymbol{\psi}$. For our weak model SDE (43), only the first seven rows of \mathbf{R}^T are non-zero, and hence only the first seven components of the new noises $\boldsymbol{\chi}$ are significant. Thus seven new noises $\boldsymbol{\chi}$, with coefficients in \mathbf{R}^T , replace the 16 noises $\boldsymbol{\psi}$.

Computer algebra [50, §9] also computes the QR factorisation of the quadratic noise coefficients in the weak model SDE (43). However, the computer algebra also handles the case of four Fourier modes, instead of the three Fourier modes used to compute (43). There is a significant difference in the amount of detail: with truncation to four Fourier modes the weak model (43) has 92 terms in its centred difference form; in comparison, with truncation to three Fourier modes the weak model (43) has 53 terms in its centred difference form. However, upon replacing the quadratic noises $\boldsymbol{\psi}$ by equivalent noises $\boldsymbol{\chi}$ the resultant weak model has complexity largely independent of the number of retained Fourier modes. The model from four Fourier modes is

$$\begin{aligned}
\dot{U}_j = & \gamma \frac{1}{h^2} \delta^2 U_j - \gamma^2 \frac{1}{12h^2} \delta^4 U_j - \gamma \alpha \frac{1}{h} U_j \mu \delta U_j \\
& + \sigma [\phi_0 + \alpha h U_j (-.2026\phi_1 + .02252\phi_3) - .02555\alpha^2 h^2 U_j^2 \phi_2] \\
& + \gamma \sigma \delta^2 (-.04167\phi_0 + .02533\phi_2) + \gamma^2 \sigma \delta^4 (.005971\phi_0 - .002752\phi_2) \\
& + \alpha h \gamma \sigma \{ \mu \delta U_j [.02533\phi_2 + \mu \delta (.05111\phi_1 - .00649\phi_3)] \\
& + \delta^2 U_j [(-.02031\phi_1 - .0001769\phi_3) + \delta^2 (.01278\phi_1 - .001622\phi_3)] \\
& + U_j [\mu \delta (.08314\phi_0 - .02533\phi_2) + \delta^2 (.02555\phi_1 - .003245\phi_3)] \} \\
& + .04681\alpha h^2 \sigma^2 \chi_1 \\
& + \alpha h^2 \gamma \sigma^2 [\mu \delta_2 (.02163\chi_2 + .02949\chi_3) \\
& + \mu \delta_1 (-.0006027\chi_2 - .000111\chi_3 + .0008305\chi_4) \\
& + \mu \delta_1 \mu \delta_2 (-.01168\chi_1 + .000587\chi_5) \\
& + \delta_2^2 (-.005875\chi_1 + .0001334\chi_5 + .0004103\chi_6) \\
& + \delta_1^2 (.001608\chi_1 - .002696\chi_5 - .0005192\chi_6 + .001116\chi_7) \\
& + \delta_1^2 \delta_2^2 (-.00292\chi_1 + .0001468\chi_5)] \\
& + .01126\alpha^2 h^3 \sigma^2 U_j \chi_2 + .01751\alpha^2 h^2 \sigma^2 U_j + \mathcal{O}(\sigma^3, \alpha^3 + \gamma^3). \tag{44}
\end{aligned}$$

In this weak model, the new noises χ_n *implicitly* have two subscripts to parametrise noise in pairs of nearby elements, as for ψ_{nmk} : these reflect some of the subtle correlations between neighbouring elements. The differences between this SDE and the previous weak model SDE (43) are the following:

- it is derived by resolving four subgrid Fourier modes within each element instead of three; for example, the effects of the subgrid microscale noise ϕ_3 explicitly appear;

- the implicit effects of the subgrid microscale noise ϕ_3 change some of the coefficients slightly—for example, the interesting mean destabilising term $.01643\alpha^2h^2\sigma^2\mathcal{U}_j$ in the SDE (43) is more accurately $.01751\alpha^2h^2\sigma^2\mathcal{U}_j$ in the SDE (44);
- the multitude of nonlinearity induced quadratic noise interactions have been replaced by just seven completely equivalent noise processes χ (although, as discussed earlier for ψ , these seven implicitly represent five times as many independent noise processes per element!).

6 Conclusion

The crucial virtue of the final weak model SDE (44), as also recognised by Just et al. [27], is that we may accurately take large time steps as *all* the fast dynamics are eliminated in the systematic closure. The critical innovation here is that we have demonstrated, via the particular example of Burgers' SPDE (1), how it is feasible to analyse the net effect of many independent subgrid microscale stochastic effects, both within an element and between neighbouring elements, in a quite general SPDE (6). Observe that we remove all memory convolutions from the model SDE and that quadratic effects in the noise processes effectively generate a mean drift and abstract effectively new noises. General formulae for modelling quadratic noise interactions [51], together with the iterative construction of stochastic slow manifold models [42], empower us to model a wide range of SPDEs.

Theoretical support for the models comes from dividing the spatial domain into finite sized elements with coupling conditions (4), invoking SCM theory [5], and then systematically analysing the subgrid processes together with the appropriate physical coupling between the elements. This approach builds on success in discretely modelling deterministic PDEs [43, 45, 32, e.g.].

We sought solutions to Burgers' SPDE (1) on a domain of size L with periodic boundary conditions so that the discrete models are homogeneous. What about other domains with physical boundary conditions at their extremes? The coupling parameter γ controls the information flow between adjacent elements; thus our truncation to a finite power in γ restricts the influence in the model of any physical boundaries to just a few elements near that physical boundary. Crucially, the approach proposed here is based purely upon the *local* dynamics on small elements while seeking to maintain fidelity with the solutions of the original SPDE. In the interior, the methods described here remain unchanged and thus produce identical model SDEs. The same methodology, but with different details can account for physical

boundaries to produce a discrete model valid across the whole domain. This has already been shown for the deterministic Burgers' PDE [46] and shear dispersion in a channel [32].

Future research may find a useful simplification of the analysis used here if it can determine the mean drift terms, quadratic in σ^2 , without having to compute the other quadratic noise terms.

This approach to spatial discretisation of the SPDE (6) may be extended easily to higher spatial dimensions as already commenced for deterministic PDEs [32, 34]. Because of the need to decompose the stochastic residuals into eigenmodes on each element, the application to higher spatial dimensions are likely to require tessellating space into simple rectangular elements for SPDEs.

A Local simple noise is impossible

This Appendix proves that we cannot reduce the number of the noise terms in the model SDE (27) without making the noises non-local. Suppose that in a model SDE such as (27) we have a noise term forcing of the form

$$\begin{bmatrix} \mathbf{a} + \mathbf{b}\delta^2 & 1 \end{bmatrix} \begin{bmatrix} \psi \\ \hat{\psi} \end{bmatrix}.$$

Seek to simplify by an orthogonal transformation to new noises $(\chi, \hat{\chi})$ by

$$\begin{bmatrix} \psi \\ \hat{\psi} \end{bmatrix} = \begin{bmatrix} Q_1 & Q_3 \\ Q_2 & Q_4 \end{bmatrix} \begin{bmatrix} \chi \\ \hat{\chi} \end{bmatrix}$$

where the Q matrix is orthogonal. Then the noise term

$$\begin{aligned} \begin{bmatrix} \mathbf{a} + \mathbf{b}\delta^2 & 1 \end{bmatrix} \begin{bmatrix} \psi \\ \hat{\psi} \end{bmatrix} &= \begin{bmatrix} \mathbf{a} + \mathbf{b}\delta^2 & 1 \end{bmatrix} \begin{bmatrix} Q_1 & Q_3 \\ Q_2 & Q_4 \end{bmatrix} \begin{bmatrix} \chi \\ \hat{\chi} \end{bmatrix} \\ &= \begin{bmatrix} (\mathbf{a} + \mathbf{b}\delta^2)Q_1 + Q_2 & (\mathbf{a} + \mathbf{b}\delta^2)Q_3 + Q_4 \end{bmatrix} \begin{bmatrix} \chi \\ \hat{\chi} \end{bmatrix}. \end{aligned}$$

The noise $\hat{\chi}$ is eliminated, and the model SDE made simpler, only when $(\mathbf{a} + \mathbf{b}\delta^2)Q_3 + Q_4 = 0$; that is,

$$Q_4 = -(\mathbf{a} + \mathbf{b}\delta^2)Q_3.$$

But the entire Q matrix must also be orthogonal. Hence, among other identities,

$$Q_1Q_2^\dagger + Q_3Q_4^\dagger = 0 \quad \text{and} \quad Q_2Q_2^\dagger + Q_4Q_4^\dagger = 1.$$

Using Q_4 then makes these

$$Q_1 Q_2^\dagger = (a + b\delta^2) Q_3 Q_3^\dagger \quad \text{and} \quad Q_2 Q_2^\dagger + (a + b\delta^2)^2 Q_3 Q_3^\dagger = 1,$$

recognising that all operator products are commutative as, in a spatially homogeneous domain, the operators are identical at each point in the spatial domain and hence the eigenvectors of the operators are identical, namely spatial discrete Fourier modes. Use the first identity to eliminate $Q_3 Q_3^\dagger$ from the second to obtain

$$\begin{aligned} Q_2 Q_2^\dagger + (a + b\delta^2) Q_1 Q_2^\dagger &= 1 \\ \Leftrightarrow [Q_2 + (a + b\delta^2) Q_1] Q_2^\dagger &= 1. \end{aligned}$$

But if Q_1 and Q_2 are to be *local* operators, then this equation can only be satisfied if both $Q_2 + (a + b\delta^2) Q_1$ and Q_2^\dagger are scalars. Hence $(a + b\delta^2) Q_1$ must be a scalar which is impossible for a *local* operator Q_1 . This contradiction proves we cannot reduce the number of noise modes in the SDE (27) while maintaining locality in the model.

I expect analogous results for more complex models, and so, for example, do not even consider simplifying the analogous noise components of the SDE (29).

References

- [1] Ludwig Arnold and Peter Imkeller. Normal forms for stochastic differential equations. *Probab. Theory Relat. Fields*, 110:559–588, 1998. doi:10.1007/s0044000050159.
- [2] A. Bensoussan and F. Flandoli. Stochastic inertial manifold. *Stochastics and Stochastics Rep.*, 53:13–39, 1995.
- [3] Nils Berglund and Barbara Gentz. Geometric singular perturbation theory for stochastic differential equations. *J. Diff. Equations*, 191:1–54, 2003. doi:10.1016/S0022-0396(03)00020-2.
- [4] D. Blomker, M. Hairer, and G. A. Pavliotis. Modulation equations: stochastic bifurcation in large domains. *Communications in Mathematical Physics*, 258:479–512, 2005. doi:10.1007/s00220-005-1368-8.
- [5] P. Boxler. A stochastic version of the centre manifold theorem. *Probab. Th. Rel. Fields*, 83:509–545, 1989.

- [6] P. Boxler. How to construct stochastic center manifolds on the level of vector fields. *Lect. Notes in Maths*, 1486:141–158, 1991.
- [7] Tomas Caraballo, Jose A. Langa, and James C. Robinson. A stochastic pitchfork bifurcation in a reaction-diffusion equation. *Proc. R. Soc. Lond. A*, 457:2041–2061, 2001. doi:10.1098/rspa.2001.0819.
- [8] J. Carr. *Applications of centre manifold theory*, volume 35 of *Applied Math. Sci.* Springer-Verlag, 1981.
- [9] J. Carr and R. G. Muncaster. The application of centre manifold theory to amplitude expansions. I. Ordinary differential equations. *J. Diff. Eqns.*, 50:260–279, 1983.
- [10] J. Carr and R. G. Muncaster. The application of centre manifold theory to amplitude expansions. II. Infinite dimensional problems. *J. Diff. Eqns*, 50:280–288, 1983.
- [11] Xu Chao and A. J. Roberts. On the low-dimensional modelling of Stratonovich stochastic differential equations. *Physica A*, 225:62–80, 1996. doi:10.1016/0378-4371(95)00387-8.
- [12] P. H. Coullet, C. Elphick, and E. Tirapegui. Normal form of a Hopf bifurcation with noise. *Physics Letts*, 111A(6):277–282, 1985.
- [13] S. M. Cox and A. J. Roberts. Initial conditions for models of dynamical systems. *Physica D*, 85:126–141, 1995. doi:10.1016/0167-2789(94)00201-Z.
- [14] G. Da Prato and J. Zabczyk. *Ergodicity for infinite dimensional systems*, volume 229 of *London Mathematical Society Lecture Note Series*. Cambridge University Press, 1996.
- [15] Giuseppe Da Prato, Arnaud Debussche, and Roger Temam. Stochastic Burgers’ equation. *Nonlinear Differential Equations and Applications*, 1(4):389–402, 1994. doi:10.1007/BF01194987.
- [16] J. Dolbow, M. A. Khaleel, and J. Mitchell. Multiscale mathematics initiative: A roadmap. Report from the 3rd DoE workshop on multiscale mathematics. Technical report, Department of Energy, USA, <http://www.sc.doe.gov/ascr/mics/amr>, December 2004.
- [17] Francois Drolet and Jorge Vinals. Adiabatic reduction near a bifurcation in stochastically modulated systems. *Phys. Rev. E*, 57:5036–5043, 1998. [<http://link.aps.org/abstract/PRE/v57/p5036>].

- [18] Francois Drolet and Jorge Vinals. Adiabatic elimination and reduced probability distribution functions in spatially extended systems with a fluctuating control parameter. *Phys. Rev. E*, 64:026120, 2001. [<http://link.aps.org/abstract/PRE/v64/e026120>].
- [19] Jinqiao Duan, Kening Lu, and Bjorn Schmalfuss. Invariant manifolds for stochastic partial differential equations. *The Annals of Probability*, 31:2109–2135, 2003. doi:10.1214/aop/1068646380.
- [20] C. Foias, M. S. Jolly, I. G. Kevrekidis, and E. S. Titi. Dissipativity of numerical schemes. *Nonlinearity*, 4:591–613, 1991. doi:10.1088/0951-7715/4/3/001.
- [21] C. Foias and E. S. Titi. Determining nodes, finite difference schemes and inertial manifolds. *Nonlinearity*, 4:135–153, 1991. doi:10.1088/0951-7715/4/1/009.
- [22] J. Fujimura. Methods of centre manifold multiple scales in the theory of nonlinear stability for fluid motions. *Proc Roy Soc Lond A*, 434:719–733, 1991.
- [23] C. W. Gear, Ju Li, and I. G. Kevrekidis. The gap-tooth method in particle simulations. *Phys. Lett. A*, 316:190–195, 2003. doi:10.1016/j.physleta.2003.07.004.
- [24] Dror Givon, Raz Kupferman, and Andrew Stuart. Extracting macroscopic dynamics: model problems and algorithms. *Nonlinearity*, 17:R55–R127, 2004. <http://stacks.iop.org/no/17/R55>.
- [25] H. Grad. Asymptotic theory of the Boltzmann equation. *Phys. Fluids*, 6:147–181, 1963.
- [26] W. Grecksch and P. E. Kloeden. Time-discretised Galerkin approximations of parabolic stochastic PDEs. *Bull. Austral Math. Soc.*, 54:79–85, 1996.
- [27] Wolfram Just, Holger Kantz, Christian Rodenbeck, and Mario Helm. Stochastic modelling: replacing fast degrees of freedom by noise. *J. Phys. A: Math. Gen.*, 34:3199–3213, 2001. doi:10.1088/0305-4470/34/15/302.
- [28] Yuri Kabanov and Sergei Pergamenshchikov. *Two-scale stochastic systems*, volume 49 of *Applications of mathematics: stochastic modelling and applied probability*. Springer, 2003.

- [29] P. E. Kloeden and E. Platen. *Numerical solution of stochastic differential equations*, volume 23 of *Applications of Mathematics*. Springer–Verlag, 1992.
- [30] E. Knobloch and K. A. Wiesenfeld. Bifurcations in fluctuating systems: The centre manifold approach. *J. Stat Phys*, 33:611–637, 1983.
- [31] T. Mackenzie and A. J. Roberts. Holistic finite differences accurately model the dynamics of the Kuramoto–Sivashinsky equation. *ANZIAM J.*, 42(E):C918–C935, 2000. <http://anziamj.austms.org.au/V42/CTAC99/Mack>.
- [32] T. MacKenzie and A. J. Roberts. Holistic discretisation of shear dispersion in a two-dimensional channel. In K. Burrage and Roger B. Sidje, editors, *Proc. of 10th Computational Techniques and Applications Conference CTAC-2001*, volume 44, pages C512–C530, March 2003. <http://anziamj.austms.org.au/V44/CTAC2001/Mack>.
- [33] T. MacKenzie and A. J. Roberts. Accurately model the Kuramoto–Sivashinsky dynamics with holistic discretisation. *SIAM Journal on Applied Dynamical Systems*, 5(3):365–402, 2006. doi:10.1137/050627733.
- [34] Tony MacKenzie. *Create accurate numerical models of complex spatio-temporal dynamical systems with holistic discretisation*. PhD thesis, University of Southern Queensland, 2005.
- [35] E. Meron and I. Procaccia. Theory of chaos in surface waves: The reduction from hydrodynamics to few-dimensional dynamics. *Phys. Rev. Lett.*, 56:1323–1326, 1986. doi:10.1103/PhysRevLett.56.1323.
- [36] R. Metzler. Non-homogeneous random walks, generalised master equations, fractional Fokker–Planck equations, and the generalised Kramers–Moyal expansion. *Eur. Phys. J. B*, 19:249–258, 2001. doi:10.1007/s100510170333.
- [37] A. Naert, R. Friedrich, and J. Peinke. Fokker–Planck equation for the energy cascade in turbulence. *Physical Rev. E*, 56:6719–6722, 1997. doi:10.1103/PhysRevE.56.6719.
- [38] National Physical Laboratory. *Modern Computing Methods*, volume 16 of *Notes on Applied Science*. Her Majesty’s Stationary Office, 1961.
- [39] P. K. Pollett and A. J. Roberts. A description of the long-term behaviour of absorbing continuous time Markov chains using a centre manifold. *Advances Applied Probability*, 22:111–128, 1990. doi:10.2307/1427600.

- [40] I. Procaccia. Universal properties of dynamically complex systems: the organisation of chaos. *Nature*, 333:618–623, 1988. 16th June. doi:10.1038/333618a0.
- [41] A. J. Roberts. Appropriate initial conditions for asymptotic descriptions of the long term evolution of dynamical systems. *J. Austral. Math. Soc. B*, 31:48–75, 1989.
- [42] A. J. Roberts. Low-dimensional modelling of dynamics via computer algebra. *Computer Phys. Comm.*, 100:215–230, 1997.
- [43] A. J. Roberts. Holistic discretisation ensures fidelity to Burgers’ equation. *Applied Numerical Modelling*, 37:371–396, 2001.
- [44] A. J. Roberts. Holistic projection of initial conditions onto a finite difference approximation. *Computer Physics Communications*, 142:316–321, 2001.
- [45] A. J. Roberts. A holistic finite difference approach models linear dynamics consistently. *Mathematics of Computation*, 72:247–262, 2002. <http://www.ams.org/mcom/2003-72-241/S0025-5718-02-01448-5>.
- [46] A. J. Roberts. Derive boundary conditions for holistic discretisations of Burgers’ equation. In K. Burrage and Roger B. Sidje, editors, *Proc. of 10th Computational Techniques and Applications Conference CTAC-2001*, volume 44, pages C664–C686, March 2003. <http://anziamj.austms.org.au/V44/CTAC2001/Robe>.
- [47] A. J. Roberts. Holistic discretisation of dynamical partial differential equations. Technical report, <http://www.sci.usq.edu.au/staff/aroberts/holistic.html>, April 2003. version 1.1.
- [48] A. J. Roberts. Low-dimensional modelling of dynamical systems applied to some dissipative fluid mechanics. In Rowena Ball and Nail Akhme-diev, editors, *Nonlinear dynamics from lasers to butterflies*, volume 1 of *Lecture Notes in Complex Systems*, chapter 7, pages 257–313. World Scientific, 2003.
- [49] A. J. Roberts. A step towards holistic discretisation of stochastic partial differential equations. In Jagoda Crawford and A. J. Roberts, editors, *Proc. of 11th Computational Techniques and Applications Conference CTAC-2003*, volume 45, pages C1–C15, December 2003. [Online] <http://anziamj.austms.org.au/V45/CTAC2003/Robe> [December 14, 2003].

- [50] A. J. Roberts. Computer algebra derives discretisations of the stochastically forced Burgers' partial differential equation. Technical report, [<http://www.sci.usq.edu.au/staff/robertsa/CA/caddsfbpde.pdf>], January 2006.
- [51] A. J. Roberts. Resolving the multitude of microscale interactions accurately models stochastic partial differential equations. *LMS J. Computation and Maths*, to appear. <http://arxiv.org/abs/math.DS/0506533>.
- [52] A. J. Roberts and I. G. Kevrekidis. Higher order accuracy in the gap-tooth scheme for large-scale dynamics using microscopic simulators. In Rob May and A. J. Roberts, editors, *Proc. of 12th Computational Techniques and Applications Conference CTAC-2004*, volume 46 of *ANZIAM J.*, pages C637–C657, July 2005. <http://anziamj.austms.org.au/V46/CTAC2004/Robe> [July 20, 2005].
- [53] G. Samaey, I. G. Kevrekidis, and D. Roose. Damping factors for the gap-tooth scheme. In S. Attinger and P. Koumoutsakos, editors, *Multiscale Modeling and Simulation*, volume 39 of *Lecture Notes in Computational Science and Engineering*, pages 93–102. Springer–Verlag, 2004.
- [54] G. Samaey, I. G. Kevrekidis, and D. Roose. The gap-tooth scheme for homogenization problems. *SIAM Multiscale Modeling and Simulation*, 4:278–306, 2005. <http://epubs.siam.org/sam-bin/dbq/article/60204>.
- [55] N. Sri Namachchivaya and Y. K. Lin. Method of stochastic normal forms. *Int. J. Nonlinear Mechanics*, 26:931–943, 1991.
- [56] M. Tutkun and L. Mydlarski. Markovian properties of passive scalar increments in grid-generated turbulence. *New J. Phys.*, 6, 2004. doi:10.1088/1367-2630/6/1/049.
- [57] Eric Vanden-Eijnden. Asymptotic techniques for SDEs. In *Fast Times and Fine Scales: Proceedings of the 2005 Program in Geophysical Fluid Dynamics*. Woods Hole Oceanographic Institution, 2005. <http://gfd.whoi.edu/proceedings/2005/PDFvol12005.html>.
- [58] Wei Wang and Jinqiao Duan. Invariant manifold reduction and bifurcation for stochastic partial differential equations. Technical report, [<http://arXiv.org/abs/math.DS/0607050>], 2006.

- [59] M. J. Werner and P. D. Drummond. Robust algorithms for solving stochastic partial differential equations. *J. Comput. Phys*, 132:312–326, 1997. doi:10.1006/jcph.1996.5638.